DEVELOPMENT OF A MYOELECTRIC DETECTION CIRCUIT PLATFORM FOR COMPUTER INTERFACE APPLICATIONS

A Thesis

presented to

the Faculty of California Polytechnic State University,

San Luis Obispo

In Partial Fulfillment

of the Requirements for the Degree

Master of Science in Biomedical Engineering

by

Nickolas Andrew Butler

March 2019

COMMITTEE MEMBERSHIP

TITLE:	Development of a Myoelectric Detection Circuit Platform for Computer Interface Applications
AUTHOR:	Nickolas Andrew Butler
DATE SUBMITTED:	March 2019
COMMITTEE CHAIR:	Robert Szlavik, Ph.D. Professor of Biomedical Engineering
COMMITTEE MEMBER:	Robert Crockett, Ph.D. Associate Dean for Innovation Infrastructure College of Engineering
COMMITTEE MEMBER:	Kristen O'Halloran Cardinal, Ph.D. Professor of Biomedical Engineering

ABSTRACT

Development of a Myoelectric Detection Circuit Platform for Computer Interface Applications

Nickolas Andrew Butler

Personal computers and portable electronics continue to rapidly advance and integrate into our lives as tools that facilitate efficient communication and interaction with the outside world. Now with a multitude of different devices available, personal computers are accessible to a wider audience than ever before. To continue to expand and reach new users, novel user interface technologies have been developed, such as touch input and gyroscopic motion, in which enhanced control fidelity can be achieved. For users with limited-to-no use of their hands, or for those who seek additional means to intuitively use and command a computer, novel sensory systems can be employed that interpret the natural electric signals produced by the human body as command inputs. One of these novel sensor systems is the myoelectric detection circuit, which can measure electromyographic (EMG) signals produced by contracting muscles through specialized electrodes, and convert the signals into a usable form through an analog circuit. With the goal of making a general-purpose myoelectric detection circuit platform for computer interface applications, several electrical circuit designs were iterated using OrCAD software, manufactured using PCB fabrication techniques, and tested with electrical measurement equipment and in a computer simulation. The analog circuit design culminated in a 1.35” x 0.8” manufactured analog myoelectric detection circuit unit that successfully converts a measured EMG input signal from surface skin electrodes to a

clean and usable 0-5 V DC output that seamlessly interfaces with an Arduino Leonardo microcontroller for further signal processing and logic operations. Multiple input channels were combined with a microcontroller to create an EMG interface device that was used to interface with a PC, where simulated mouse cursor movement was controlled through the voluntary EMG signals provided by a user. Functional testing of the interface device was performed, which showed a long battery life of 44.6 hours, and effectiveness in using a PC to type with an on-screen keyboard.

TABLE OF CONTENTS

Page

LIST OF TABLES

Table Page

LIST OF FIGURES

Figure Page

Chapter 1

INTRODUCTION

1.1.1 General Introduction to Electrophysiology and Biopotentials

In the broad field of electrophysiology, the detection, measurement, and analysis of bioelectric potentials, or biopotentials, are the fundamental topic of focus. These electrical signals are generated from excitable cells found in muscular, nervous, and glandular tissue, and possess membrane voltage-gated ion channels that control the flow of K^+, Na^+, and Cl^- ions into and out of the cell [1]. Due to differences in concentration of these charged ions inside and outside of the cell, a difference in voltage resides across the membrane. This difference in voltage is known as the resting membrane potential, which typically resides within a range of -50 mV to -100 mV for mammalian peripheral muscle excitable cells [1]. When an electrical potential stimulus is applied to the excitable cell, from either an external source, or from another nearby excitable cell, the voltage-gated ion channels will open and allow for the flow of ions into and out of the cell. This flow of ions depolarizes the intracellular membrane potential and creates what's known as an action potential as seen in figure 1.

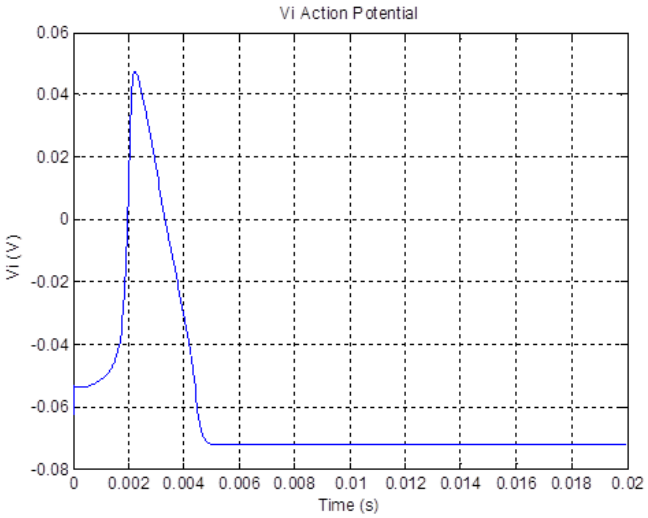

Figure 1: Intracellular membrane voltage as a function of time for an action potential

During depolarization, the intracellular membrane potential generally approaches a maximum value of +60 mV, which is known as the Nernst Potential. As the action potential is generated, it also travels along the length of the cell, which can be considered a conducting electrical impulse. For cells such as neurons, which possess axons up to several feet in length, the action potential may travel a significant distance as it conducts [2]. Therefore, to produce meaningful actions at the termination source, action potentials can travel at speeds up to 270 miles per hour [3]. To help maintain electrical continuity, and improve conduction velocity, neurons are encased in a specialized fatty membrane known as a myelin sheath [3]. Immediately after action potential production, the excitable cell may not generate additional action potentials for a duration known as the refractory period, which is controlled by membrane channel proteins with gating time constants [1]. The ultimate destination of the conducting impulse is either to the brain through a sensory neuron, or to skeletal or cardiac muscle through a motor neuron [2]. When both sensory

and motor neurons cluster together, they form nerves, which then travel to large skeletal muscle groups throughout the body.

1.1.2 Electromyography

One of the terminal sites for motor neurons is a skeletal muscle fiber, which connects via a structure known as a neuromuscular junction [2]. When an action potential travels down the neuron to the neuromuscular junction, an electrochemical cascade follows that eventually results in additional voltage-gated ion channels on the muscle fiber opening, and initiates an action potential within the muscle fiber itself. As the action potential propagates along the muscle fiber, it initiates a process known as excitation-contraction coupling, which as the sliding filament theory states, creates a muscle fiber contraction [2].

In the case of muscle fiber contraction, the motor neuron and muscle fibers operate as a single unit. This combination of a single motor neuron and all individual muscle fibers it innervates form a structure known as a motor unit [2]. For a muscle such as the biceps brachii, a motor unit typically composes 150 individual muscle fibers. The functional motor unit, beginning at the ventral horn of the spinal cord, traveling through the neuronal axon, and ending at a muscle fiber, can be seen in figure 2 below.

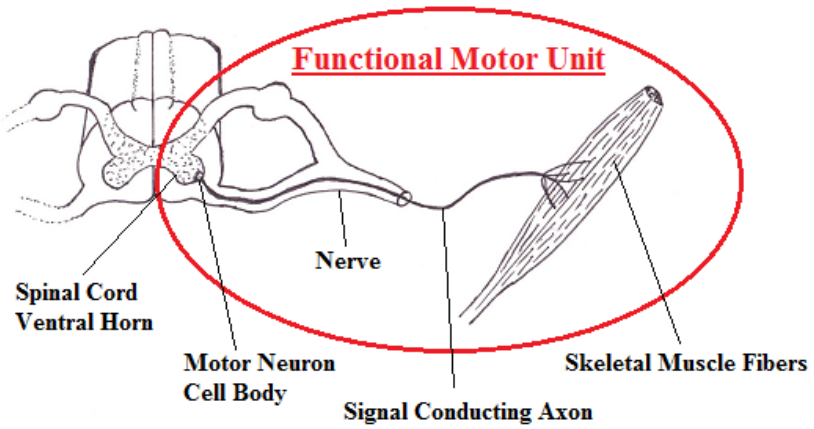

Figure 2: Functional Motor Unit

When a single motor unit is stimulated for contraction, the action potential that propagates through the muscle fibers has an amplitude of 20-2000 μV, and a discharge frequency of 6-30 Hz [1]. For peripheral skeletal muscle, the voltage potential from the motor units can be measured through a process known as electromyography or EMG [1]. To stimulate the muscle to produce a larger contractile force, more individual motor units are activated simultaneously in a process known as motor unit recruitment [2]. This subsequent increase in force production through motor unit recruitment in turn produces a proportional increase in voltage potential at the muscle.

1.1.3 Muscle Force Production and EMG Signal Intensity Relationship

In a study conducted by Liping Qi et al titled, "Spectral properties of electromyographic and mechanomyographic signals during isometric ramp and step contractions in biceps brachii", the relationship between muscle force production and EMG signal intensity was measured in an effort to characterize motor unit recruitment. An experiment was conducted involving twenty healthy subjects, in which the biceps

brachii of the non-dominant arm was the primary muscle of investigation. Using a mechanical support fixture, the subject's arm was oriented in the extended supinated position, while maintaining an elbow angle of 150°. A force transducer (Omega Engineering) was connected perpendicular to the length of the arm at the wrist to measure force production resulting from bicep flexion. To measure the EMG signal generated at the bicep, 12 mm stainless steel surface electrodes were placed midline of the biceps brachii and interfaced with a custom-built amplifier circuit connected to a laptop running Agilent VEE Pro for data collection. The testing setup can be seen in figure 3 below [4].

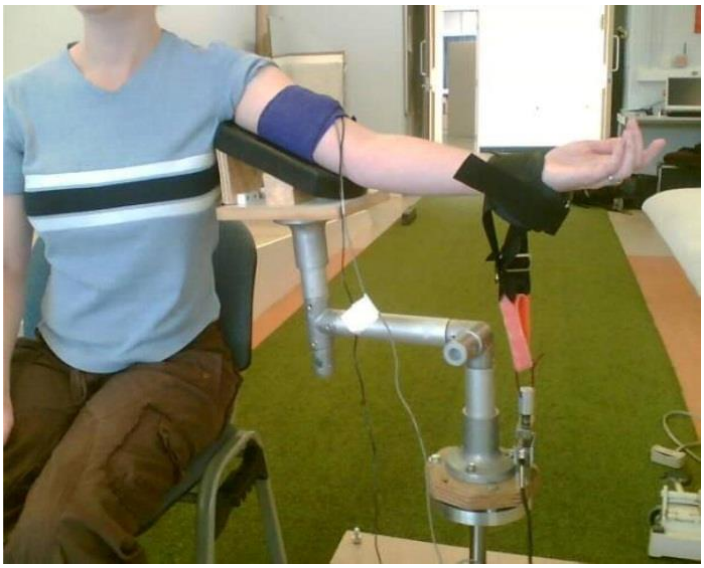

Figure 3: Force production vs. EMG signal intensity test setup [4]

To first calibrate the measurement equipment, subjects performed a maximum voluntary contraction of the biceps, which was standardized as the 100% contraction level relative to baseline. The first test performed involved using a visual feedback system to show force production, while performing a biceps flex in 20% incrementing contraction levels for 10 seconds at each increment while EMG signal intensity and force production were

measured. Increments were continued until 80% of the maximum contraction level was reached. The second test was known as the ramp test, in which subjects were instructed to gradually increase biceps brachii contraction level until 90% of the maximum contraction level was achieved. After collecting data from the entire sample group, the resulting relationship between muscle force production and EMG signal intensity for both tests was evaluated. The resulting plot of EMG signal intensity relative to force production can be seen in figure 4 below [4].

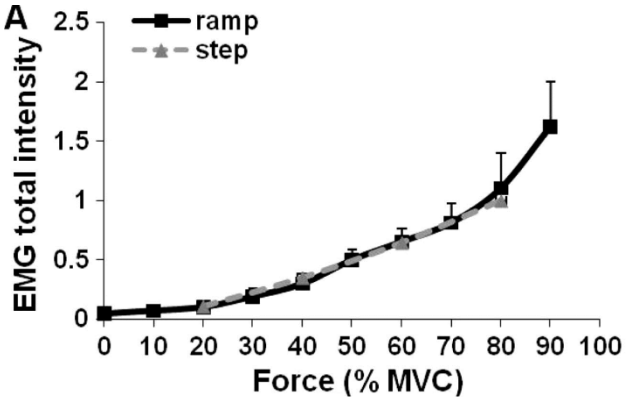

Figure 4: EMG Signal Intensity vs. Force Production [4]

Evaluating the resulting relationship between the measured EMG signal intensity and the produced force from contraction of the biceps brachii, it was observed that a relatively linear relationship existed for both the step and ramp testing conditions. Overall, the results obtained in the study conducted by Liping Qi et al suggest that when specifically measuring EMG signal amplitude, an accurate estimate of muscle contraction effort can be predicted. By capturing an EMG signal at its source, a processed form of this signal could serve as input to a wide variety of voluntary control systems. In addition to use as a

binary input, the amplitude of the signal could also be measured and compared to a known threshold to generate a dynamic output signal.

1.1.4 Types of Electrodes for EMG Signal Capture

Classically, the method of capturing the EMG signal of a conducting muscle of moderate volume is through the use of a conducting electrode. The two primary EMG capture methods are surface EMG (type A), which uses surface electrodes, and intramuscular EMG, in which needle electrodes are inserted directly into the muscle fibers (type B). These two methods can be seen in figure 5 below.

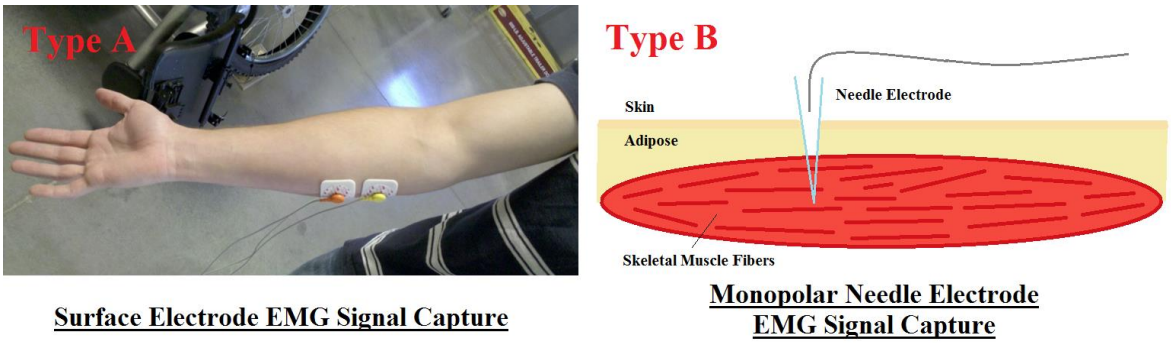

Figure 5: Surface and Intramuscular EMG Capture Techniques

Characteristic differences between these two techniques influence the type setting in which they can be used. For surface EMG, typically mechanical clamping electrodes or disposable adhesive electrodes are used (figure 6).

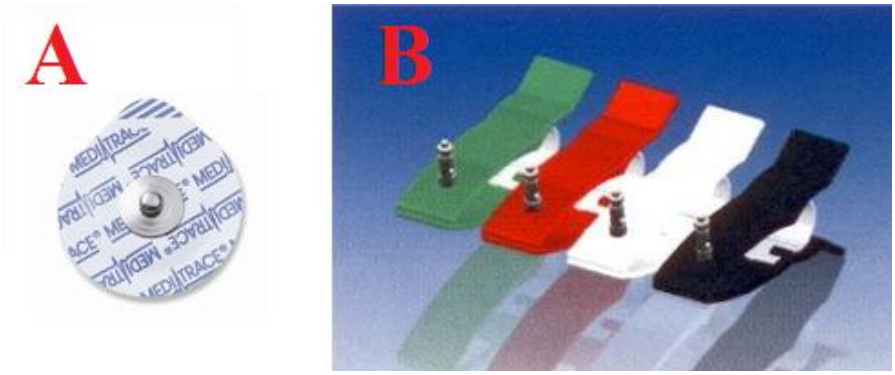

Figure 6: Types of Surface Electrodes [Danlee Medical Products, 2011]

Disposable adhesive electrodes are composed of some kind of conducting metal, such as Ag/Ag Chloride, and a conducting adhesive hydrogel. While surface electrodes are non-invasive and easy to use, they are sensitive to electrical signals over a large area and can only be used with superficial muscles. This large detection area can create difficulties when attempting to isolate EMG signals from individual muscles, as signals from other nearby contracting muscles can be picked up as well. For intramuscular EMG, individual or deeper muscles can be better distinguished through the use of needle electrodes. While this technique has much greater detection precision and much lower impedance than surface EMG, the technique is fairly invasive and can be uncomfortable for the user [2]. In regard to EMG readings from arm muscles, a clear signal is defined as: that which conveys information about the individually contracting muscle motor units. Clear and differentiable signals can be read via indwelling needle electrodes; however, they are not ideal for long-term signal capture, due to their potential for infection. In a study conducted by Jin Lee et al., contractile motor unit signal optimization was performed by analyzing several different surface electrode configurations using an advanced volume conductor model in combination with an intracellular action potential equation to

simulate individually contracting motor units under the skin. Seven different spatial filters (electrode configurations) were evaluated using this model, with the criteria that the best signal was that which presented the most differentiable motor unit action potential signal relative to two individual motor units. It was found that the bi-transverse double differential electrode configuration (figure 7) was able to capture the most distinguishable individual motor unit signals [5]. This study described how a differential electrode configuration is important for isolating a usable signal from contracting muscles.

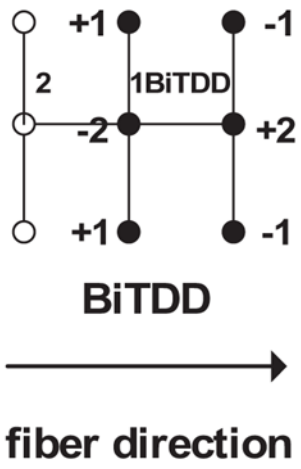

Figure 7: Bi Transverse Double Differential Electrodes [5]

1.1.5 Impedance Characteristics of Skin

For EMG detection using surface electrodes, it is important to understand the inherent electrical characteristics of skin. In a study conducted by S.J. Dorgan and R.B. Reilly titled, “A model for human skin impedance during surface functional neuromuscular stimulation,” an updated mathematical model of the dynamic electrical

characteristics of human skin was created through an experiment involving neuromuscular stimulation. After completing the experiment, it was found that skin has linear and non-linear impedance characteristics due to the variability of epithelial composition. A recreation of the equivalent circuit model can be seen below:

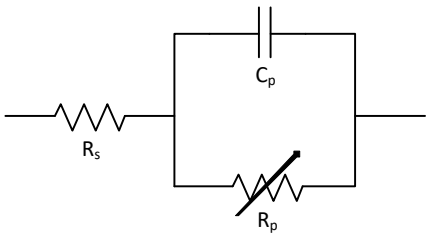

Figure 8: Equivalent Non-Linear Circuit Model for Skin

Referencing the equivalent model above, R_s represents the linear impedance component due to dermis and subcutaneous layers, while C_p and R_p represent the non-linear RC component due to the epidermis. The variability for R_p was found to be influenced primarily by the relative thickness of the epidermal layer [6].

Regarding the actual impedance variability of skin, a study conducted by J. Rosell et al measured skin impedance while varying signal frequency from 1 Hz to 1 MHz. Measurements were taken on the leg, forehead, and thorax of ten subjects, where no skin preparation was conducted (no abrasion to lower skin impedance) other than the application of a conducting gel. Results showed that for low frequency signals, skin impedance varied from 10 kΩ to 1MΩ, and for high frequency signals, impedance was found to be in the hundreds of ohms. Based on the high input impedance of skin at lower frequencies, it was concluded that the design of biopotential amplifiers incorporate very high input impedances to reduce the amount of noise picked up from a differential measurement source [7].

1.2.1 Biopotential Amplifiers and the Myoelectric Circuit

When detecting EMG signals either through the surface or intramuscular method, some form of analog signal processing is required to make the signal readable by measurement equipment. Typically, this processing is done through an electronic circuit known as a biopotential amplifier, or in the case specifically for EMG signals, a myoelectric circuit. For EMG signals measured at the muscle, amplitude typically range from 0 to 10 mV AC (peak-to-peak) or 0 to 1.5 mV (rms), however when measuring with surface electrodes, the large skin impedance can lower the signal to 0 to 2 mV AC [8]. In order to convert this signal to a range that is more easily interfaced with measurement systems, amplification of the signal is generally performed by an analog amplifier, such as an inverting or non-inverting amplifier circuit. Another important circuit is the differential amplifier, which rejects the common mode signal attributed to noise.

Regarding the frequency spectrum of EMG signals, they encompass a usable spectrum of 0-500 Hz, with the majority of usable signal falling within the 50-150 Hz range [9]. When measuring EMG within this active spectrum however, a number of sources of interference effectively degrade the overall quality of the signal. Electromagnetic radiation sources such as radio transmissions, power outlets, electrical wires, and fluorescent lights operate with a primary frequency of 60 Hz at amplitudes up to three times the inherent EMG signal [9]. When measuring with surface electrodes, the wires and metal contacts effectively act as antennas, picking up these sources of interference. In addition to interference from outside sources, another source of interference, known as motion artifacts, are destructive signals generated by motion at the electrode/skin interface, and through flexing of the electrode cable. Interference signals

from this source reside within the 0 to 20 Hz range. To significantly reduce the impact of these sources of electrical interference and improve the overall quality of the EMG signal, several different electrical circuits can be implemented. The first circuit commonly utilized is the differential amplifier, which uses a two-source electrode design, in combination with a ground reference, and allows for a significant amount of the noise to be eliminated through a process known as common mode signal rejection.

Another circuit commonly used to remove the unwanted noise from sources operating at higher frequencies is the active filter circuit. Active filter circuits include: active low pass, active high pass, and when combined, active band pass filters. The primary benefit from using active filters is that they not only allow for discrimination of the allowed frequency, but can implement a signal gain as well. For applications with small potential EMG signals, this is an advantageous characteristic. High pass and low pass filters function by only allowing a specific bandwidth to pass through the circuit, while all other frequencies are filtered out. The desired passing bandwidth can be specifically set by adjusting the resistive and capacitive values for the circuit. With the previously mentioned EMG active frequency of 0-500 Hz, and 0-20 Hz interference due to motion artifacts, it would be permissible to design a band pass filter with a passing bandwidth of 20-500 Hz. To remove the common interference produced from lights, power outlets, and other electronics that operate at 60 Hz, another filtering technique known as band reject filtering can be used. This technique incorporates what is known as a notch filter to remove specific frequencies with a very narrow bandwidth.

To operate as a controller interface, it is also important to convert the inherent AC EMG signal to a DC signal. This operation can be performed through the use of an active

rectifier circuit. More information on the analog circuit components that perform these amplification, filtering, and rectifying operations can be found later in section 1.3.1.

When these circuit elements are combined into a single circuit, they form the principle basis for the myoelectric circuit. A block diagram for the general form of EMG systems can be seen in figure 9 below.

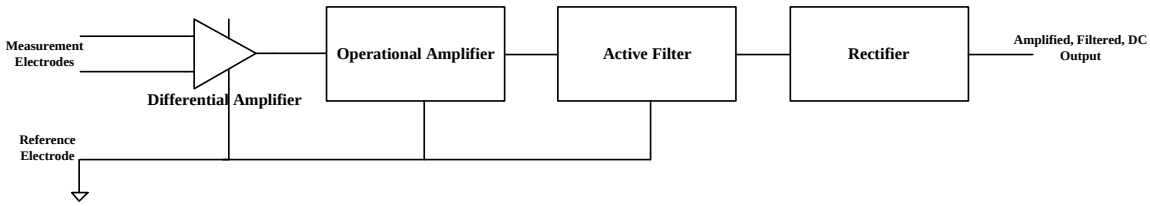

Figure 9: General Form of the Myoelectric Recording System

1.2.2 Applications of the Myoelectric Circuit

The fundamental purpose of the myoelectric system is to capture EMG signals, and transform them into a form that can be interfaced with other electronic devices. This inherent ability to act as a user interface facilitates numerous practical applications in areas such as prosthetics, robotics, computer interaction, and assist devices. For disabled individuals, the myoelectric interface method presents a means to increase mobility and dexterity. Specifically, with prosthetics, a patient who has undergone an amputation of an arm or a hand can regain a high degree of manual dexterity through the control of robotic systems via captured EMG signals produced from residual voluntary muscle groups in the arm. By capturing the signals from these residual muscle groups, specifically the ones that formerly performed the now lost action, such as closing one's hand, a highly intuitive user control system can be developed. As seen with the several current myoelectric prosthetic hands in the market, such as the DEKA Research "Luke" arm, Touch Bionics'

"iLimb", and the "DARPA Hand", the use of this control system has proven to be highly effective. Figure 10 below shows the DARPA hand in use.

Figure 10: The DARPA Hand Using Myoelectric Interface [Mike McGregor, 2009]

1.2.3 Signal Processing and Machine Learning

For applications in which complex coordinated motion is desired, such as power grasp, wrist flexion/extension, lateral pinch, cylindrical grasp, etc., multiple input channels are required to interpret these complex signals. Each of these input channels would typically be isolated to an individual muscle, and in the case of most practical EMG detection methods, measured through the use of two surface electrodes. To reliably interpret complex motions measured from several inputs, a microprocessor is commonly utilized in conjunction with an analog amplifying circuit to create an EMG signal recognition system. An optimized EMG recognition system should only accept and process target patterns that reflect the intended motion, and reject those that do not [10]. In a study conducted by Yi-Hung Liu et al titled, "Towards a high-stability EMG

recognition system for prosthesis control A one-class classification based non-target EMG pattern filtering scheme", the authors highlighted that the variable accuracy and stability of these EMG recognition systems is a critical issue that often leads to unintended motion for myoelectric prosthesis users. They identified that other myoelectric detection systems relied on an EMG recognition method known as a "multi-class classifier", which would classify and label inputs performed during a calibration training phase. This training phase would classify the input pattern into pre-defined "motions", such as those listed above. However, there would often be unaccounted motions that the user intended to perform, such as those with variation in signal amplitude or combination. In a study conducted by Thilina Lalitharatne et al, the effects of muscle fatigue due to prolonged prosthetic were found to significantly diminish EMG-based signal amplitude [11]. In these situations, the resulting motion of the prosthetic device would either be unintended, or diminished. To allow for a wide variety of motions to be detected, with flexibility and adaptability in mind, the authors presented an advanced machine-learning non-target pattern filtering technique (NTPF). This pattern filtering technique was based on a method known as "one-class classification" or "novelty detection", where a limited data-set of EMG target patterns recorded during a training phase could be utilized to identify patterns that existed outside of an exact "class". This method used a machine-learning mathematical technique called "support vector data description" (SVDD), in which the data-set recorded during training would be used to generate a mathematical hypersphere with a minimum volume. The boundary of this hypersphere would be utilized to identify target data. After deriving expressions for the center point and radius of the hypersphere, an expression for the volume of the

hypersphere, and probability that an input would reside in a certain space was established. By treating the volume expression as in constrained optimization problem, eventually a decision function for the SVDD was established:

$$D_{\mathrm{SVDD}}(\mathbf{x}) = c - 2\sum_{\mathbf{x}_i \in \mathrm{SVs}} \alpha_i K(\mathbf{x}, \mathbf{x}_i)$$

Figure 11: SVDD decision function [10]

Where c is a constant that relates the radius and total volume occupied by the hypersphere, α_i is a component of the data point vector that describes location relative to the hypersphere boundary, K is the kernel function that describes the dot product data point vector array, and x is the target EMG pattern. In cases where $D_{SVDD}(x) \leq 0$, the target EMG pattern was accepted as x. When the condition wasn't true, the pattern was identified as "non-target" and therefore rejected.

For the purpose of their study, the SVDD data analysis method was limited to a single EMG input pair. Therefore, they utilized two different hyperspheres to evaluate the data. The overall structure of the non-target pattern filtering technique and EMG recognition system can be seen in figure 12 below:

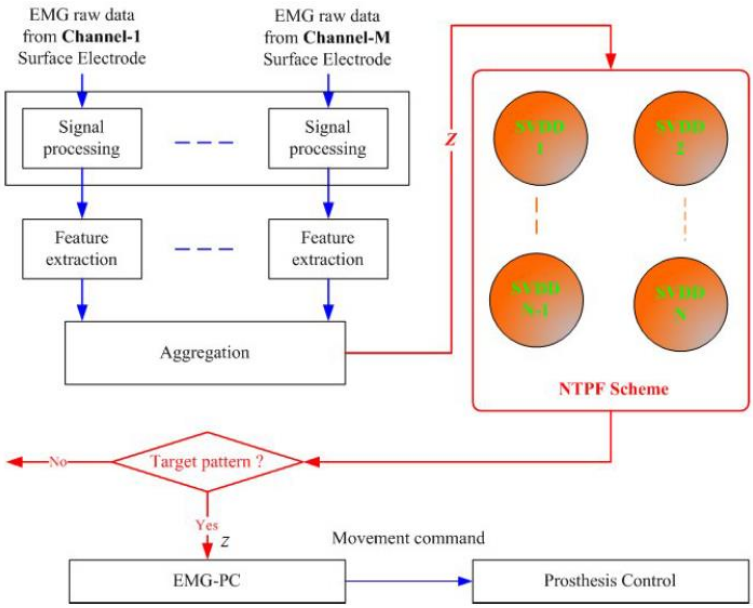

Figure 12: EMG Recognition System with NTPF [10]

To evaluate this filtering technique relative to traditional multi-class classifier techniques, Yi-Hung Liu et al constructed a myoelectric detection circuit that utilized EMG surface electrodes for signal capture. Real time signal processing was carried out using a 60 Hz notch filter and a 30-400 Hz band-pass filter. The data was fed to an AD converter that sampled at 2.5 KHz, and transferred the data to a PC. Next, four components from each EMG input's raw data were selected, and compiled into a vector data array. The two vector data arrays were then combined, and fed into the NTPF routine, and evaluated using the SVDD decision function. If the pattern was found to be targeted, it would then be processed by a traditional decision tree known as the EMG pattern classifier (EMG-PC), which would then generate the appropriate prosthetic motion. For the purposes of this study, a five-fingered table-top mechanical hand was utilized to establish credibility of the EMG recognition system. A user would hook up two electrode pairs to their arm, perform an intended hand motion, and if measured and

identified correctly, the mechanical hand would replicate the motion. The set-up can be seen in figure 13 below:

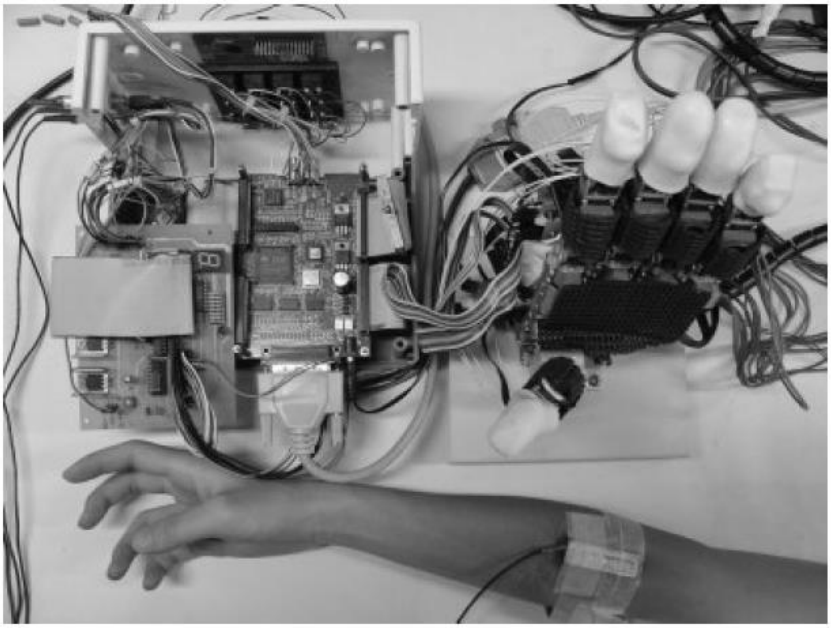

Figure 13: EMG processing module with mechanical hand [10]

Eight kinds of hand motions were identified, each of which was recorded for the training routine 10 times. Following training, the user was assigned a randomized motion routine. Over the course of the test routine, each motion was performed a total of 10 times. After performing the test using the NTPF recognition scheme, the test was repeated using a traditional multi-class classifier technique, which instructed processed signals to be passed directly to the EMG pattern classifier. Results showed a significant difference in the successful classification rates between the two methods. The NTPF recognition scheme was found to be successful 87% of the time, while the traditional multi-class classifier technique proved to be successful only 51% of the time.

In summary, this study conducted by Yi-Hung Liu et al proved that with significant machine learning and processing, relatively high interpretation accuracy rates

could be achieved. However, the sampling rate used in this study produced extremely large data sets that took significant time to process. The authors state that while the technique was effective in improving EMG signal interpretation reliability, the processing duration required to produce an output was sufficiently long, such that the scheme would not currently be practical for prosthetic control. Reducing the time to process the data was to be their main focus for future work [10].

As outlined with this study, it will be necessary for an EMG detection system to incorporate user calibration data in addition to standard analog signal processing to produce usable outputs. Since the motions evaluated in the study by Yi-Hung Liu et al were somewhat complex and measured through only two electrode pairs, perhaps using several inputs could be reliably interpreted through simpler motions combined with additional electrode inputs.

1.3.1 Analog Circuit Components

The following section provides additional background of several circuit elements commonly found in EMG detection circuits.

1.3.2 The Differential Amplifier

The differential amplifier, also known as a difference amplifier, is arguably one of the most important analog elements of the myoelectric detection circuit. This element actively rejects noise from surrounding lights, computers, power lines, and other electromagnetic sources, which are picked up by the body and electrical leads [9]. It does so through the use of two input electrodes, used in conjunction with a ground reference. The circuit is designed in such a way that the component of the signal that is different

between the two inputs is amplified and passed through, while the component that is the common is rejected. In the case of EMG detection, the differential signal is from the contracting muscle, while the common signal is from noise. Off-the-shelf amplifiers often come with a rating known as a "common mode rejection ratio", or "CMRR", with the rating given in dB. CMRR is defined in the equation below:

$$CMRR = 10log_{10}\left(\left|\frac{A_d}{A_c}\right|\right)^2$$

In this equation, A_d is the gain of the differential component of the amplifier, while A_c is the gain of the common mode component. As A_c goes to zero, the CMRR goes to infinity [1]. For myoelectric signal detection, it is typically recommended to use operational amplifiers that have a CMRR of 90 dB or greater [9]. A diagram of a differential amplifier, with the connection methods can be seen in the image below:

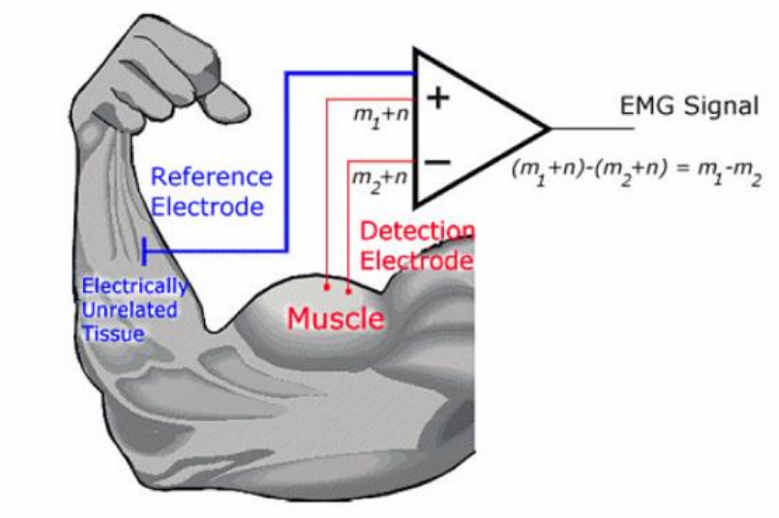

Figure 14: A configured differential amplifier interface [12]

As the diagram shows, the detecting electrodes connected to the positive and negative terminals of the differential amplifier are also connected to the target muscle. A third

electrically unrelated terminal is connected as the reference, or ground. In the diagram, *m* is the muscle signal, while *n* is the noise. The signal passed into the rest of the circuit is given by:

$$(m_1 + n) - (m_2 + n) = m_1 - m_2$$

A simulated version of a differential amplifier coupled to two voltage following buffer amplifier circuits can be seen in the picture below.

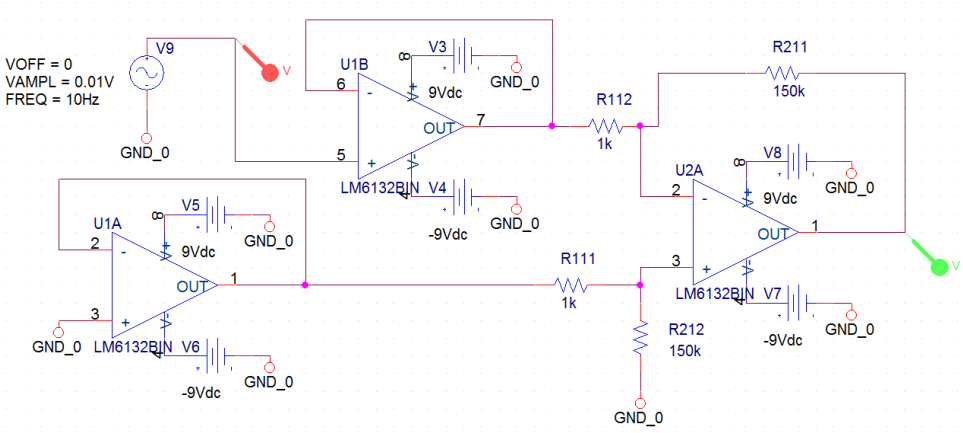

Figure 15: A Simulated Differential Amplifier Circuit

When used in EMG detection cases, adding a voltage following buffer amplifier can be helpful in reducing the transfer of high input impedance to the rest of the circuit. Without this addition, the high input impedance of an electrode would attenuate the active differential gain, $A_{d,}$ of the proceeding differential amplifier.

1.3.3 Active Band-Pass Filter

Another circuit useful in further eliminating noise from EMG signals is the band-pass filter. This filter combines both a low-pass, and a high-pass filtering circuit to create a circuit block that attenuates all outgoing signals except those that fall within a pre-set frequency spectrum. The high pass filter only attenuates components of the signal that fall in the low frequency range of 20 Hz and below. When built with an operational amplifier, the circuit can not only filter, but actively amplify the signal when coupled with an operational amplifier. To set the active gain and low pass threshold of this circuit, resistor and capacitor values may be selected, and evaluated according to the function describing the output voltage with respect to frequency shown below,

$$V_o(j\omega) = -V_i(j\omega)\frac{R_{f-HP}}{R_{i-HP}}\frac{j\omega R_{f-HP}C_{f-HP}}{1 + j\omega R_{f-HP}C_{f-HP}}$$

where the ratio of resistors $R_{f\text{-}HP}$ and $R_{i\text{-}HP}$ set the active circuit gain. With some manipulation, $C_{f\text{-}HP}$ can be isolated and solved for to determine capacitor value necessary to set a high pass cut-off frequency limit specified by ω.

To attenuate high frequency noise, the low pass filter can be utilized. As with the high pass circuit, incorporating an operational amplifier can add additional gain, which is necessary due to the low incident amplitude of most EMG signals. The output voltage as a function of the circuit frequency ω can be seen in the equation below,

$$V_o(j\omega) = -V_i(j\omega)\frac{R_{f-LP}}{R_{i-LP}}\frac{1}{1 + j\omega R_{f-LP}C_{f-LP}}$$

where the ratio of resistors $R_{f\text{-}LP}$ and $R_{i\text{-}LP}$ set the active circuit gain. As with the high pass filter, $Cf_{\text{-}LP}$ may be found to configure the desired low-pass cutoff frequency. A diagram of a band-pass filter can be seen in figure 16 below.

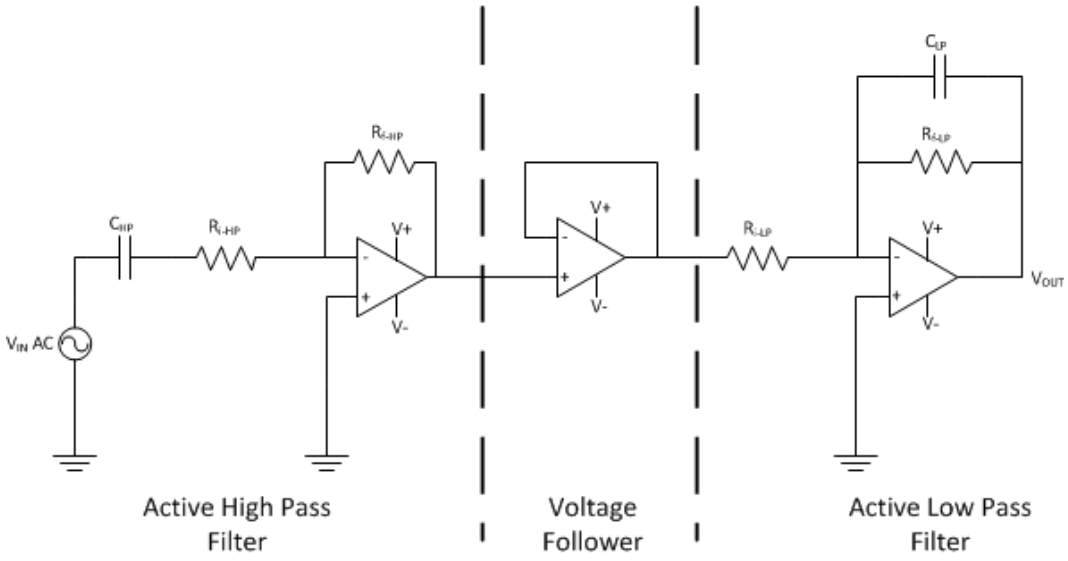

Figure 16: Band Pass Filter Circuit

1.3.4 Active Full Wave Rectifier

Due to the sinusoidal AC nature of EMG signals, an active full wave rectifier can be used in an EMG circuit to generate an analog DC signal that can easily be measured and interpreted by a microprocessor. A diagram of an active full wave rectifier can be seen in figure 17 below.

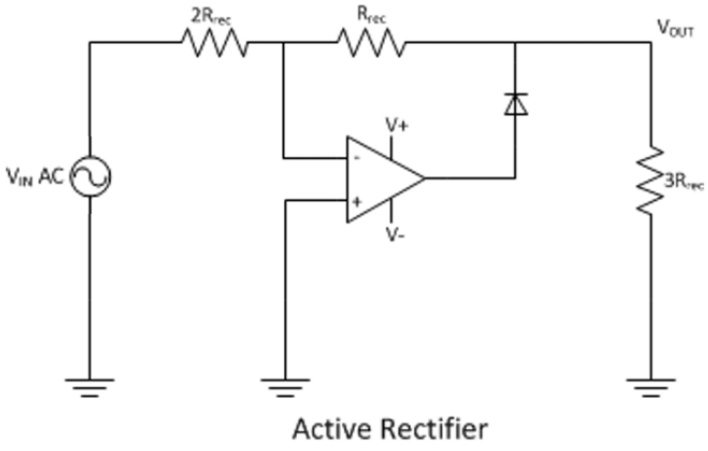

Figure 17: Active Full Wave Rectifier Circuit

This circuit functions by first acting as a voltage divider when V_{IN} is positive. This is due to the diode creating an open circuit, where current is only allowed to travel through resistors $2R_{Rec}$, R_{Rec}, *and* $3R_{Rec}$. The function for a positive waveform input signal is given by the following expression:

$$V_o = V_i \frac{1R_{Rec} + 2R_{Rec}}{1R_{Rec} + 2R_{Rec} + 3R_{Rec}} = \frac{1}{2} V_i$$

Next, when V_{IN} becomes negative, the op-amp becomes active, the diode closes, and the circuit acts as an inverting amplifier, therefore making V_{OUT} positive. The equation for a negative waveform input is shown below.

$$V_o = -V_i \frac{1R_{Rec}}{2R_{Rec}} = -\frac{1}{2} V_i$$

1.4.1 Introduction to the Arduino Microcontroller and Programming Environment

To create a functional output from a measured EMG signal, a method of analyzing and processing that signal into a meaningful output is required. This can be achieved through the use of a microcontroller electronics board, which is a small computer that can perform a host of tasks, such as processing input and output signals, performing logic operations and mathematical calculations, and read and write data. These desired tasks are coded into the microcontroller through software that is written into the onboard memory. For the purposes of EMG signal analysis, a microcontroller electronics board can easily interface with multiple discrete analog circuits simultaneously to process the measured signal for a desired means.

One such microcontroller electronics board platform that has gained significant popularity amongst hobbyists and inventors is the Arduino Electronics Platform. This

platform is open-source, in that the coding and hardware platforms, and numerous coding guides and examples are provided for free use on the internet. No matter the Arduino electronics board selected, the hardware and software are easy to understand and use.

An Arduino program is called a “sketch”, and is comprised of code that closely follows C and C++ programming languages. This allows anyone with a basic familiarity of these languages to easily create sketches of their own [13].

For projects that interface with a PC, the Arduino Leonardo electronics board is desirable, as it has built-in USB communication features. These features allow the microcontroller to easily connect with a PC and act as a virtual keyboard, mouse, or serial/COM device. The central processing unit for this board is an ATmega32u4 microchip, which allows for communication with 20 digital input/output pins, 12 of which can act as analog inputs. This board runs at 16 MHz, has a discrete micro USB connection, power input, reset button, and several LED lights [14]. The layout of this board can be seen in figure 18 below.

Figure 18: The Arduino Leonardo Microcontroller [14]

1.5.1 Summary and Aim of Thesis

In the field of electronic sensors and measurement systems, the myoelectric detection circuit, which can measure and interpret the voltage potentials generated from contracting muscles in the body, presents opportunities to interface with the human body in novel and interesting ways. For individuals with limited or no use of their hands, but who have a wish to use personal computers, an EMG measurement and interface device specifically configured, could allow them to do so. In addition to disabled individuals, this EMG interface device could also provide a novel means for anyone to interact with and use a computer, and provide more degrees of input than generally available.

The general aim of this thesis project is to do just that; create a specifically designed EMG measurement device that interfaces with a personal computer, and allows for voluntary user control. This device would incorporate a general-purpose analog myoelectric detection circuit that would perform the real-time signal isolation, filtering, and amplification required for a clean and usable EMG signal. The physical user interface would utilize surface electrodes that would easily configure to target the specific muscle groups of interest. Signal processing and recognition techniques, as well as serial I/O communication with the computer, would be accomplished using an integrated Arduino Leonardo microcontroller. Overall, the device would be intuitive to use, self-contained, and provide a means to use a personal computer in ways unlike those of traditional methods.

Chapter 2

SPECIFICATIONS

2.1.1 EMG Interface Device Introduction

The following section details the general requirements and specification of the EMG interface device. These specifications describe the design elements and rationale for this device, starting with the selected PC input interface, target user input and muscle groups, measurement electrode configuration, analog circuit elements, and digital signal processing and PC I/O. The information presented here will form the foundation from which the physical manufactured EMG interface device will take shape.

2.1.2 PC Input Specifications

When interfacing with a PC, there are several methods reading input from a user, such as a keyboard, mouse, or joystick, etc. The Arduino Leonardo microcontroller can simulate all three of these by loading the desired library file, and connecting through a USB interface. For the purposes of this EMG interface device, it is desirable to simulate hardware that maximizes the number of use cases for the user's input. Most PCs today provide a wide array of accessibility options, such as an on-screen keyboard where text can be "typed" out using a PC mouse as shown in figure 19 below.

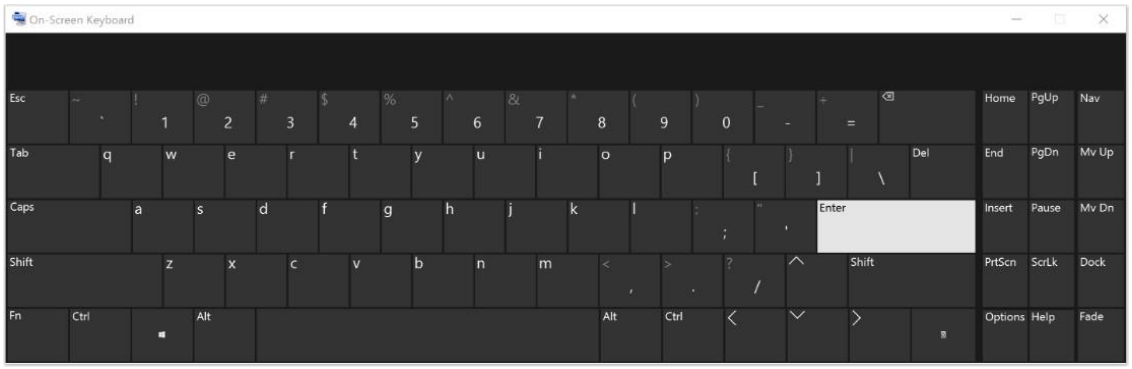

Figure 19: Example of PC On-Screen Keyboard

For this reason, movement of a mouse cursor, with the ability to "left click", was selected as the input method to simulate for the EMG interface device.

For an easy-to-understand mouse movement system, it is necessary to have enough EMG signal channels such that all cursor degrees of freedom can be generated. To accomplish this, the device user's forearm was targeted. The wrist motions shown in figure 20 below would generate an EMG signal at the target activator muscle (figure 21), and would be captured by one of four input electrode channels.

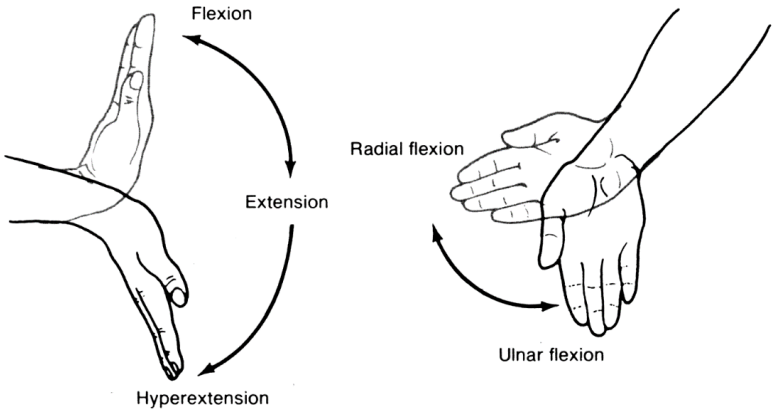

Figure 20: Targeted movements for EMG signal capture [15]

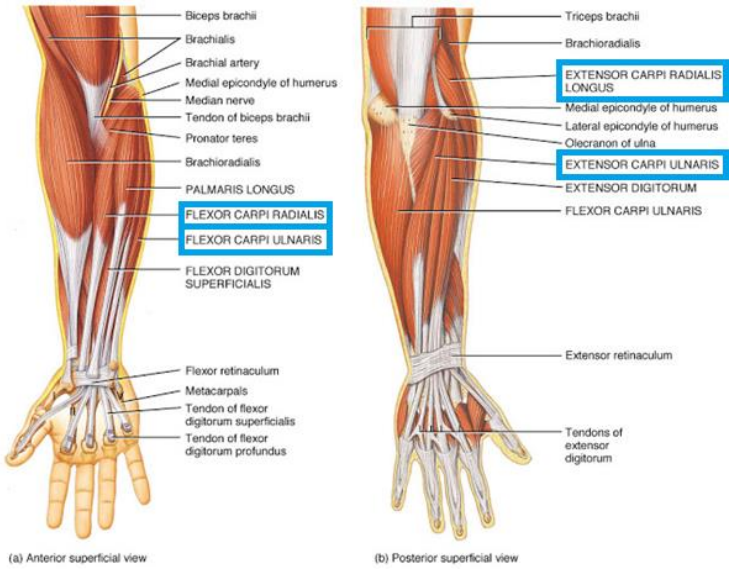

Figure 21: EMG Channel Target Muscles [16]

Table I below summarizes the cursor direction, intended wrist motion, and target activated muscle group for each EMG measurement channel.

Table I: Summary of target motion for each EMG signal

Channel	Cursor Direction	Intended Wrist Motion	Target Activated Muscle
1	Up	Radial Flexion	Extensor Carpi Radialis
2	Down	Ulnar Flexion	Flexor Carpi Ulnaris
3	Left	Flexion	Flexor Carpi Radialis
4	Right	Extension	Extensor Carpi Ulnaris

2.1.3 Measurement Electrode Configurations

To accurately isolate and detect EMG signal patterns corresponding to input directions across a user's forearm, an array of electrodes will be required. For ease of installation and general user comfort, disposable adhesive-backed surface electrodes shall be used as part of the EMG interface device. These electrodes will be placed in adjacent

pairs parallel to the length of the target muscle, such that a differential signal can be measured between both electrodes. As presented in previous sections, this differential electrode configuration, when coupled with a differential amplifier circuit, allows for the desired part of the signal (EMG) to be amplified, while the undesired electrical noise is attenuated. All measured signals shall be referenced to electrical ground of the user, through the use of a single surface electrode connected to an EMG-inactive region of the body. While the use of surface electrodes will limit signal detection to superficial muscle groups, a calibration routine shall be employed that will identify and establish EMG signal activation thresholds for each target muscle.

2.1.4 Myoelectric Circuit Analog Unit Specifications

For this EMG interface device, each input channel shall be captured and processed by a discrete myoelectric circuit unit. This unit will read a 1-10 mV 50-150 Hz AC EMG signal across two surface electrodes placed at the target muscle, amplify the differential component of the signal, and reject the common-mode through the use of an instrumentation amplifier with a CMRR of 80 dB or greater. Next, the signal will pass through an active band-pass filter, where further signal processing will amplify the EMG signal with a passing bandwidth of 20-500 Hz, and attenuate all other components attributed to noise. Next, an active full wave rectifier will convert the AC signal to DC and provide additional circuit gain. Finally, a non-inverting op-amp will provide final gain tuning to ensure a 0-5V DC signal is transferred to the microprocessor. A block diagram of the myoelectric circuit unit can be seen in figure 22 below.

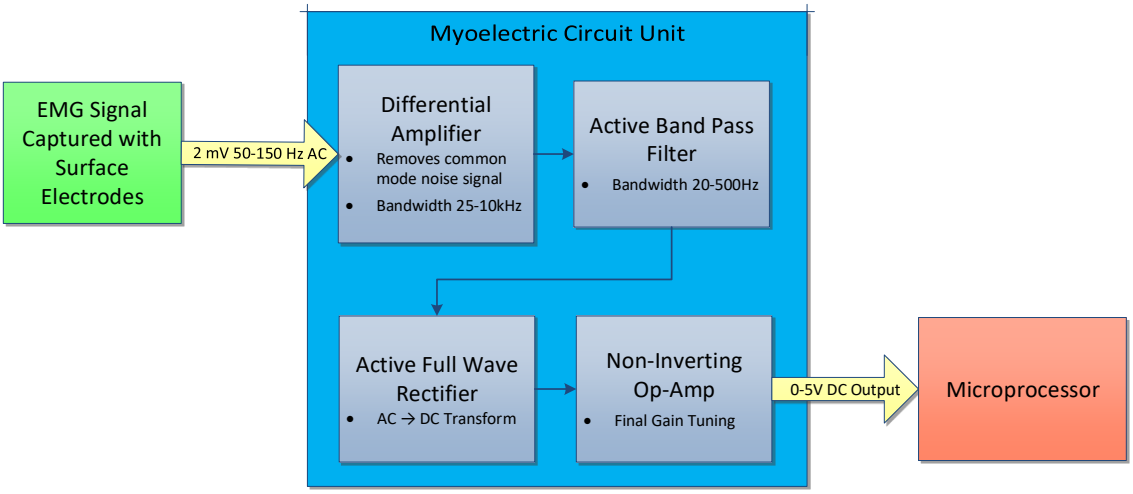

Figure 22: Myoelectric Circuit Unit

2.1.5 Microprocessor and PC Interface

For movement of the mouse cursor in all four directions, each of the myoelectric circuit units will process one EMG channel, and pass this DC signal to a discrete analog input of an Arduino Leonardo microcontroller. This microcontroller will interpret the incoming 0-5V DC analog EMG signal, and convert it to a digital Boolean value. This digital value will first be used to calibrate the input threshold where mouse cursor movement will begin. Once this value has been established, an EMG signal input greater than the threshold will trigger mouse cursor movement. This movement command will be transmitted to the PC via USB serial I/O. Figure 23 below shows a block diagram for the overall EMG interface device, comprising four discrete input channels.

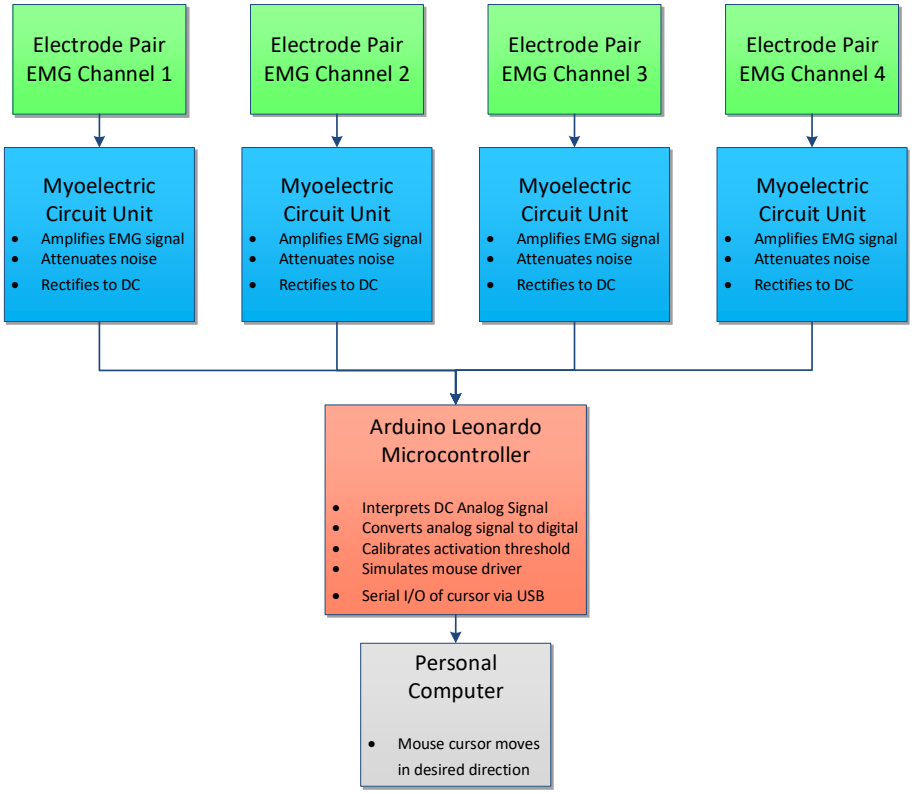

Figure 23: Block Diagram for PC EMG interface Device

2.1.6 Summary of EMG Interface Specifications

As presented in this chapter, the EMG interface device will employ an electrical circuit, where EMG signals will be captured at target muscle groups via discrete analog circuit units. These analog circuit units will connect to a surface electrode pair and measure AC EMG signals, which will then be filtered, amplified, and rectified to DC using operation amplifiers, resistors, capacitors, and diodes. Next, an Arduino Leonardo microcontroller will read the DC EMG signal supplied by the analog circuit unit, and compare the value to a calibrated threshold. When this value exceeds the threshold, the microcontroller will command a PC, connected via USB, to move a mouse cursor in the user's desired direction.

Chapter 3

DESIGN AND METHODS

3.1.1 Interface Design Introduction

Utilizing the general specifications for the EMG interface device, a circuit design layout was created with general parameters assigned. To confirm the function of circuit elements and parameters selected, testing was performed in simulated and physical circuits. The results of these tests ultimately influenced the part selection and manufacturing of the final interface device.

Upon confirming the various design elements, several fabrication processes were employed to create a functioning device. Details about the device design and assembly, components used, and manufacturing processes employed will be presented in this chapter.

3.2.1 Myoelectric Circuit Unit Simulation with PSpice

A simulation of the myoelectric sub-circuits was created in OrCAD PSpice to evaluate signal gain through resistor selection, signal filtering, and overall circuit function. For this test, a LM6132 operation amplifier model was selected due to its large gain potential and CMRR of 100 dB. Resistor and capacitor values were selected for the gain and filtering frequency desired using the governing equations listed in chapter 1.

3.2.2 Differential Amplifier

A differential amplifier was constructed in OrCAD Spice with a single 10 mV VSIN 10 Hz AC source connected to an op-amp to simulate an EMG input source. The second input op-amp terminal was wired to ground. The reason these were set at two different potentials was to simulate a differential source signal. LM6132 op-amps were used and connected to +9V DC and -9V DC power supplies. A target gain of 150 was set by connecting 150K and 1K resistors. A diagram of the simulated differential circuit can be seen in figure 24, and a summary of the voltage and resistor values can be found in table II below.

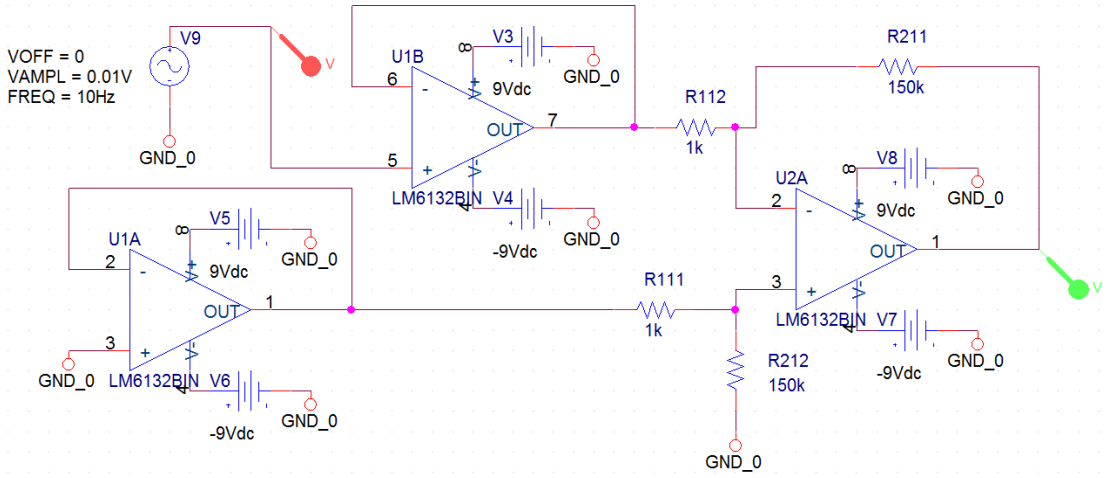

Figure 24: Differential Amplifier

Table II: Voltage and resistor values for simulated differential amplifier

Source	Value	Units
VSIN Amplitude	0.01	V
VSIN Frequency	10	Hz
Op-Amp Supply	±9	V
R111	1k	Ω
R112	1k	Ω
R211	150k	Ω
R212	150k	Ω

When running a transient simulation for 1 second, with a time step of 1ms, the following response was observed showing the input *V(V9:+)*, and output *V(R211:2)* voltages. This response can be observed in figure 25 below.

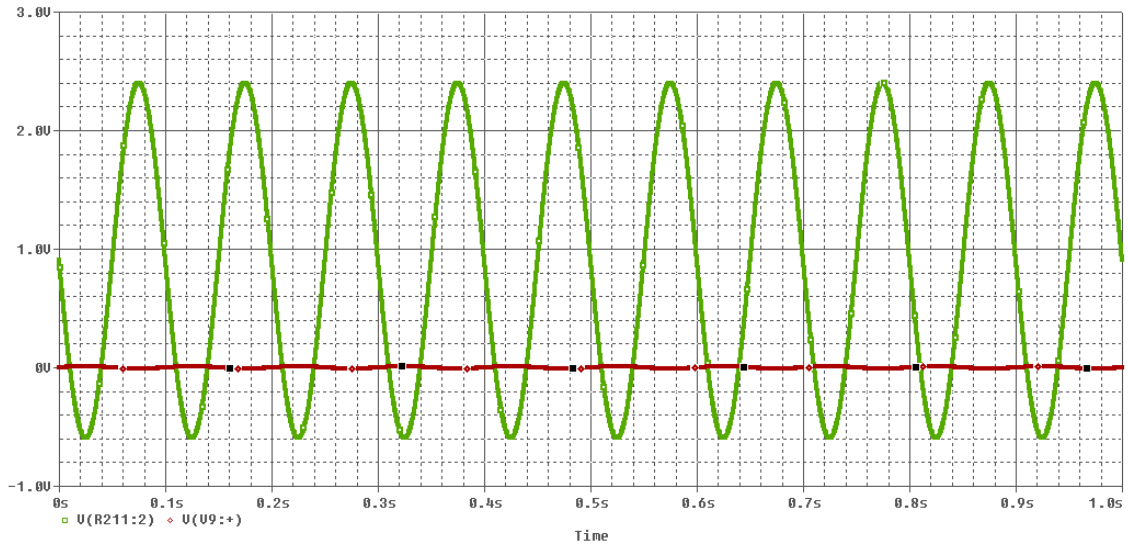

Figure 25: Transient response for Differential Amplifier

When observing the transient response for the differential amplifier, a clear amplification of the AC portion of the input signal (red) can be seen relative to the output

(green). While the output signal was observed to be centered around +0.9 V due to an inherent characteristic of the LM6132 op-amp model, the relative input and output amplitudes can be compared to determine the total circuit gain. This op-amp gain, A_{Diff} can was calculated as shown below.

$$A_{Diff} = \frac{(2.5V - .9V)}{0.01\,V} = 160$$

To confirm the concept of differential amplification, in which the common signal shared between both inputs (known as the common-mode signal) is rejected and only the difference between the two (differential mode signal) is amplified, an additional VSIN AC input was connected to the second input terminal. This second input had the same parameters as the first input, and therefore formed a common-mode signal. Figure 26 shows the modified circuit.

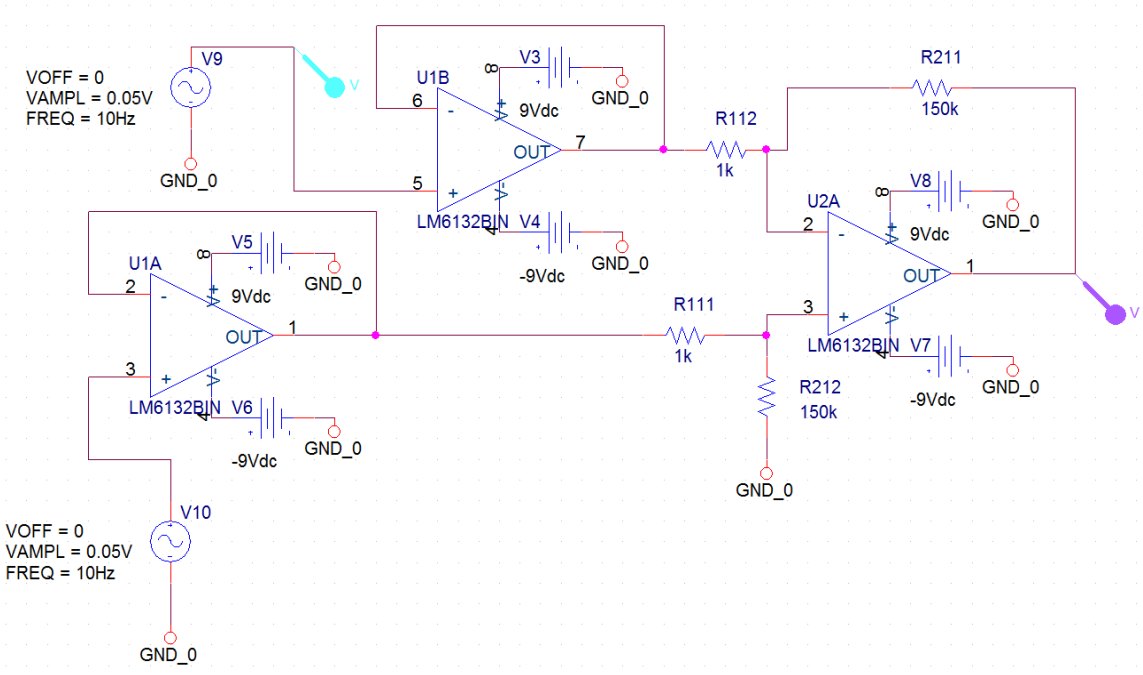

Figure 26: Differential amplifier with common-mode source

Another transient response plot was generated to demonstrate the effect of the common-mode source. Figure 27 shows the resulting input vs. output characteristics.

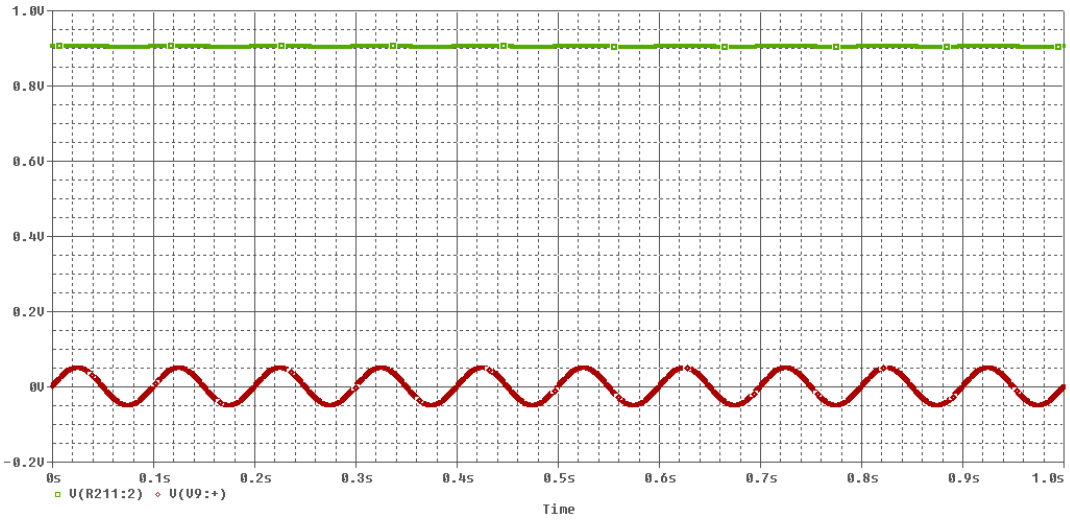

Figure 27: Transient response of common-mode source

In evaluating the transient response, it is observed that when both inputs of the differential amplifier are the identical, the AC portion of the signal is not amplified. More specifically, the red input AC voltage *V(V9:+)* can be seen to have no corresponding amplification in the green output *V(R211:2)* voltage. Again, it is important to note that the cause of the +0.9 V shift of the output signal from 0 V is attributed to the LM6132 op-amp used.

3.2.3 Band Pass Filter

For the purpose of additional filtering, a band-pass filter was simulated using the LM6132 op-amp model. The selection of the filtering bandwidth was set to 20-500 Hz, as EMG signal frequencies have been observed to fall within this range. For this circuit, all other electronic interference, which typically occurs in the range of 1 kHz and greater, should be filtered out. Again, a 10 mV AC source was selected. The LM6132 op-amps

were connected to +9V DC and -9V DC power supplies, and a target gain of 100 was set by selecting resistor pairs with factor of 10 increases at both the high-pass and low-pass portions of the circuit. C_{HP}, and C_{LP} were selected by rearranging the governing equations listed in chapter 1, and solving for their values based on the desired cutoff frequencies. The resulting band-pass filtering circuit can be observed in figure 28 and the values of resistors and capacitors selected can be found in table III below.

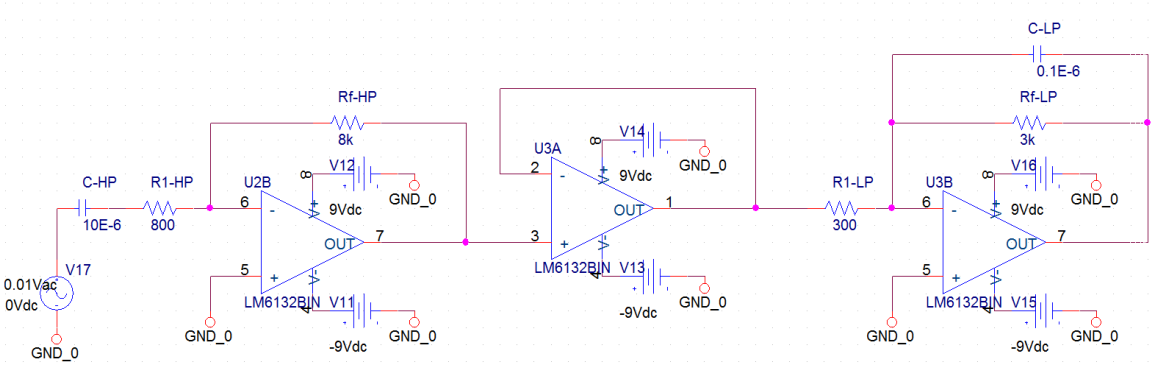

Figure 28: Band-Pass Filter Circuit

Table III: Voltage, resistor, and capacitor values for simulated band-pass filter

Source	Value	Units
VAC	0.01	V
CHP	10 x 10-6	F
R1HP	800	**Ω**
RfHP	8k	**Ω**
R1LP	300	**Ω**
RfLP	3k	**Ω**
CLP	0.1 x 10-6	F

To observe the resulting frequency spectrum from this circuit design, an AC sweep was simulated with a frequency range of 1 to 10 kHz, where frequency was plotted on a logarithmic scale. The resulting plot can be seen in observed in figure 29 below.

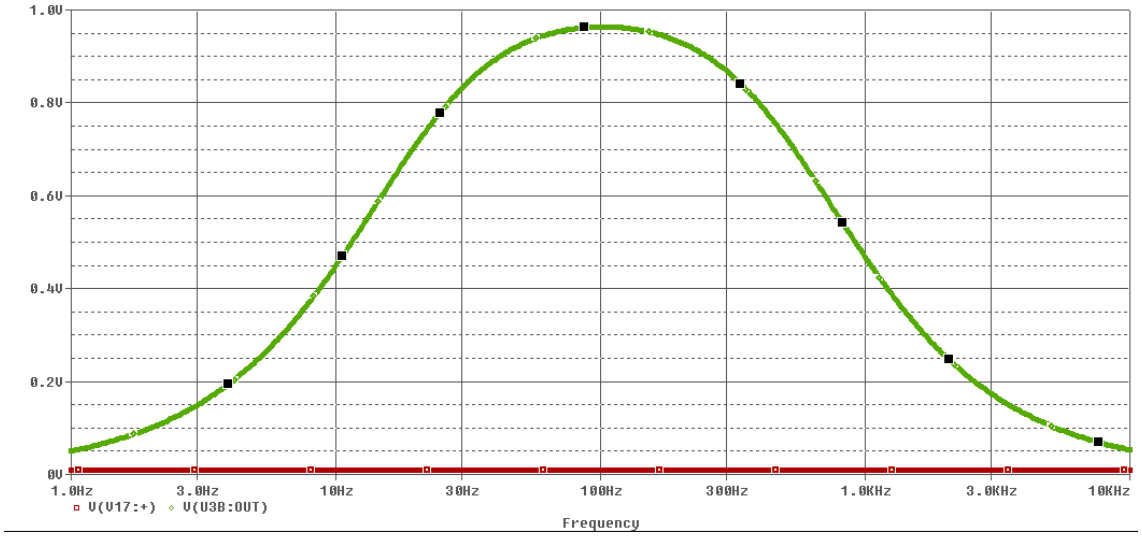

Figure 29: Frequency spectrum for band-pass filter in Voltage vs. Log(Frequency)

The resulting waveform of voltage vs. log(frequency) for the input (red) versus the output (green) was found to follow a normal distribution. The output was observed to show an amplified signal primarily within the 20-500 Hz range, with all other frequencies being attenuated. When plotted on a linear scale, the operating band-width can better be observed (figure 30).

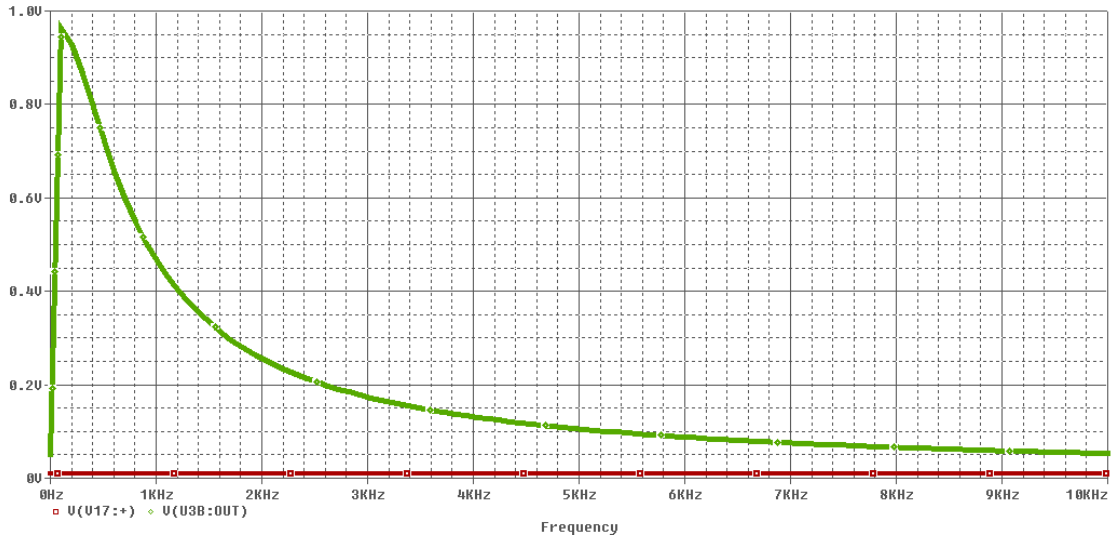

Figure 30: Frequency spectrum for band-pass filter in voltage vs. Frequency

3.2.4 Active Full Wave Rectifier

To transform the negative portion of the AC input signal to positive, an active full wave rectifier was simulated using an LF411 op-amp model. Resistor values were selected according to the governing equations listed in the introduction, such that the gain of the rectified output signal (1/2) would be consistent, and independent of the sign (positive or negative) of the input signal. A 5V AC source VPULSE was created to generate the input waveform, and, and the output was measured across the *3Rr* resistor. The active full wave rectifier circuit can be observed in figure 31 below, and the values of resistors selected can be found in table IV below.

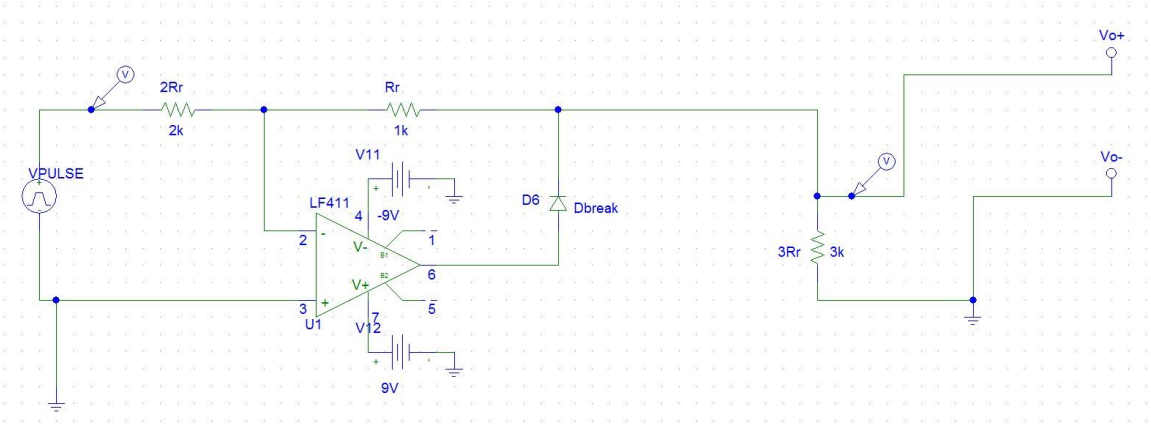

Figure 31: Active Full Wave Rectifier Circuit

Table IV: Voltage and resistor values for simulated full wave rectifier

Source	Value	Units
VPULSE	5	V
2Rr	2k	**Ω**
Rr	1k	**Ω**
3Rr	3k	**Ω**

When running a transient simulation for 100 ms, with a time step of 5 ms, the following response was observed showing the input *V(2Rr:1)*, and output *V(3Rr:2)* voltages. This response can be observed in figure 32 below.

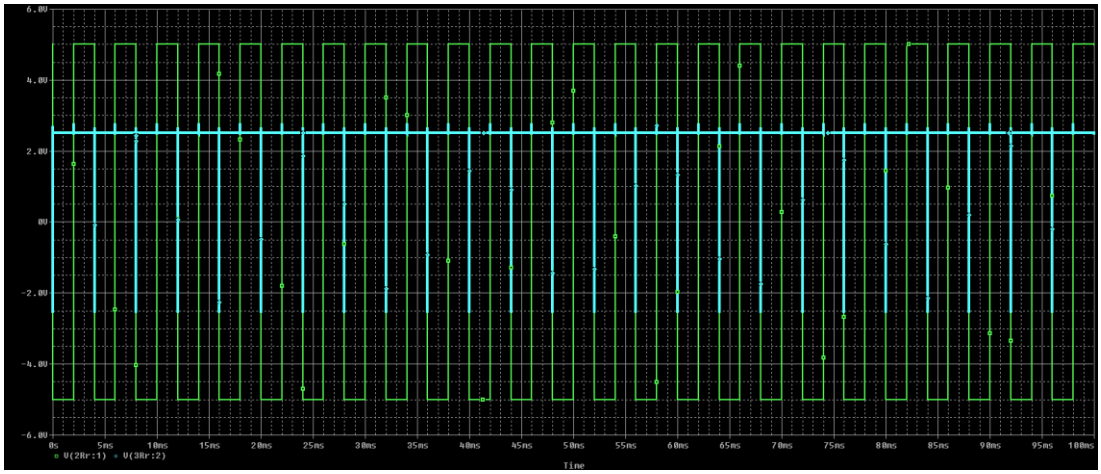

Figure 32: Transient response rectified signal

Evaluating this transient response, the output signal *V(3Rr:2)* shown in blue was observed to follow a DC trending at 2.5 V, when an AC input waveform *V(2Rr:1)* of 5 V, shown in green was applied. This confirms intended circuit gain of 0.5 when the input signal is positive, and -0.5 when the input signal is negative.

3.3.1 Myoelectric Circuit Unit Fabrication

The following section details the iterative design, prototyping, and manufacturing process of the myoelectric circuit unit.

3.3.2 Breadboard and Protoboard Circuits

After simulating the differential amplifier, band pass filter, and full wave rectifier circuit elements in PSPICE and confirming the desired output signal characteristics were

achieved, a physical circuit was constructed according to the circuit layout shown in figure 33 below.

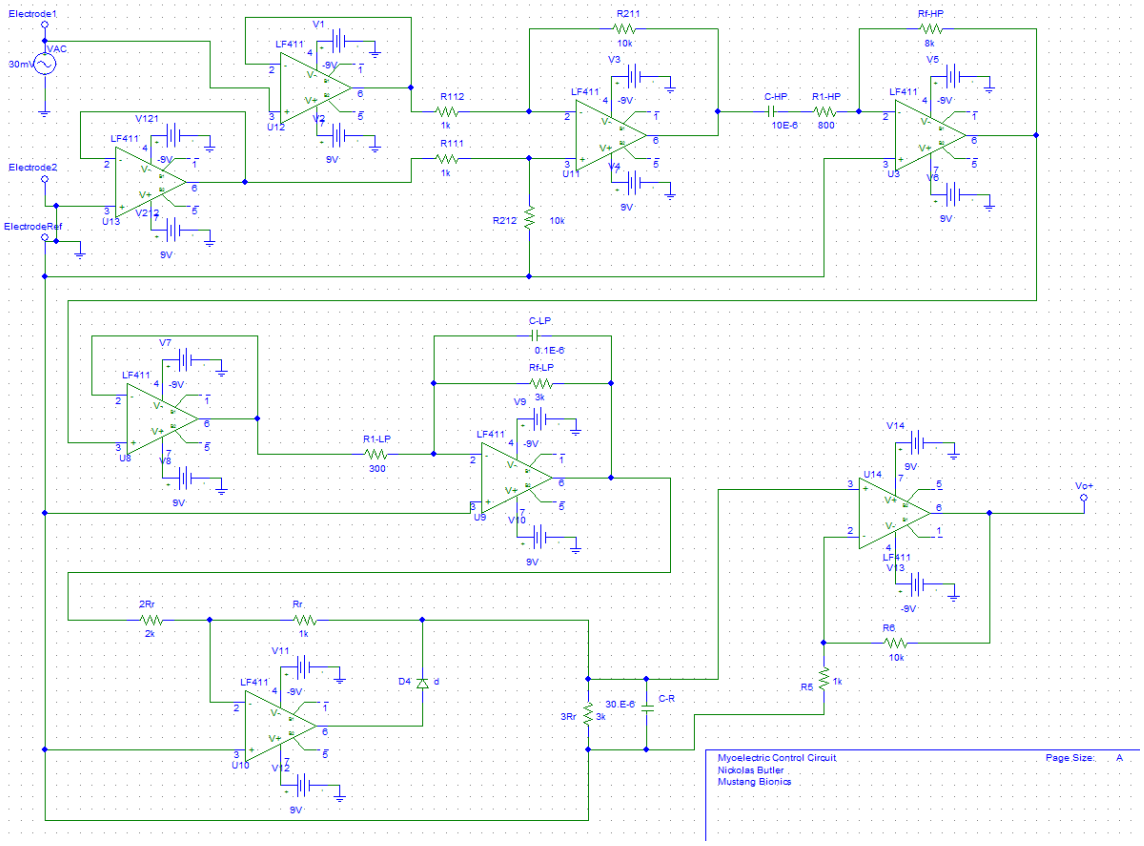

Figure 33: Myoelectric Circuit Unit Diagram

Referencing the layout above, a physical circuit was constructed first on a solderless breadboard, then on a masked and soldered prototyping board. Resistor values were selected to provide a total maximum circuit signal amplification, A_{MCU}, of 5000. This selection was made assuming a 1.0 mV input EMG signal, and a desired output of 0-5 V to operate within the measurement range of the Arduino Leonardo Microcontroller. A calculation of the total circuit gain can be seen below.

$$A_{MCU} = \frac{V_o}{V_i} = \frac{R_{F-Diff}}{R_{1-Diff}} \cdot \frac{R_{F-HP}}{R_{1-HP}} \cdot \frac{R_{F-LP}}{R_{1-LP}} \cdot \frac{1R_{Rec} + 2R_{Rec}}{1R_{Rec} + 2R_{Rec} + 3R_{Rec}} \cdot \frac{R_{F-Tune}}{R_{1-Tune}}$$

$$= \frac{10k\Omega}{1k\Omega} \cdot \frac{8k\Omega}{800\Omega} \cdot \frac{3k\Omega}{300\Omega} \cdot \frac{1k\Omega + 2k\Omega}{1k\Omega + 2k\Omega + 3k\Omega} \cdot \frac{10k\Omega}{1k\Omega} = 5000$$

To provide effective signal filtering passband of 20-500 Hz, capacitor values were selected according to the PSPICE simulations performed. The constructed and soldered prototyping board circuit can be observed in figure 34 below.

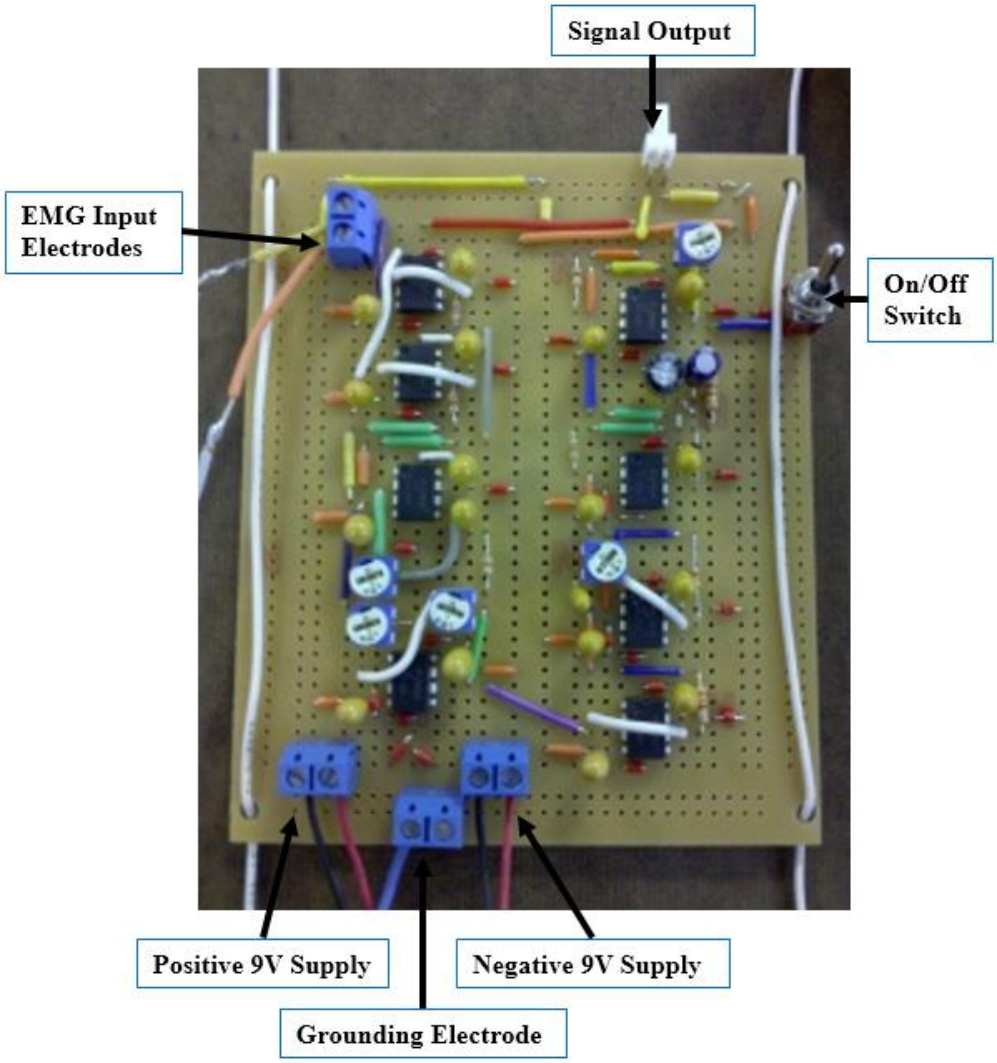

Figure 34: Myoelectric Circuit Unit Prototype

To provide the analog signal gain for this circuit, general purpose Texas Instruments LF411 operational amplifiers were used throughout this circuit. These amplifiers proved to be ideal for this circuit due to their high input impedance (10^{12} Ω), low input offset voltage, low supply current (2 mA), and large gain bandwidth [17]. The LF411 op-amp and pin layout can be seen in figure 35 below.

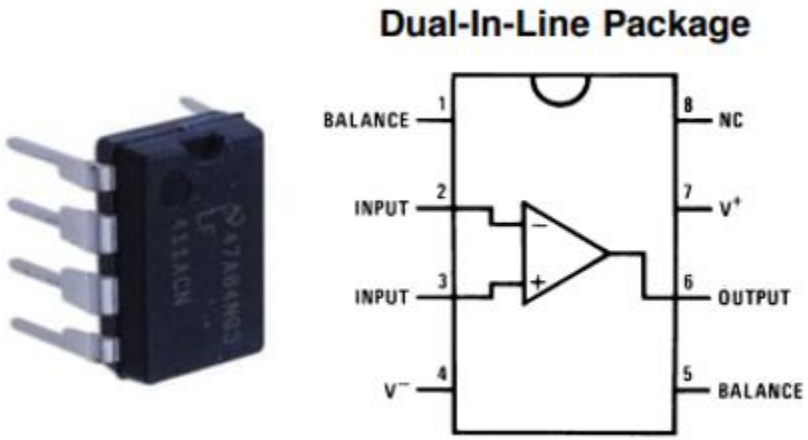

Figure 35: TI LF411 Operational Amplifier [17]

Each op-amp was supplied power to both the positive and negative rails through the use of two 9V batteries. To help eliminate power fluctuations, 10 µF capacitors were connected to each power rail supply.

The signal gain present in each circuit block was adjustable through the use of 0-10kΩ potentiometers, and signal output could be toggled on and off with a dual-pole switch. Input signals were picked up via surface electrodes placed at the target muscle, and a reference electrode was connected to circuit ground.

To confirm circuit construction, two input electrodes were placed on the biceps brachii, with one reference electrode placed on the triceps brachii. Next the output of the

circuit was connected to an analog multimeter, which was set to DC voltage measure mode. Upon voluntary contraction of the biceps muscle, a peak output signal was observed in the 1-5 V DC range, as shown in figure 36 below.

Figure 36: EMG test of Breadboard Prototype Circuit

3.3.3 PCB Circuit Design

After building the breadboard prototype circuit and confirming the circuit functions as intended, a second version of the myoelectric circuit unit was created with the goal of reducing circuit complexity, reducing power draw, reducing size, and improving the circuit assembly and construction. To achieve these goals, a printed circuit board (PCB) was designed using software Express SCH and Express PCB from the online company Express PCB. Once the circuit layout was constructed in the Express SCH software, it was then linked to the Express PCB software, where physical wiring connections to each circuit element (resistors, capacitors, op-amps, etc.) were made. After finishing the wiring diagram on a 1.5” x 2.5”, double sided PCB, the linked SCH

schematic was used to verify all connections. Finally, the completed PCB layout was purchased and ordered through the software. The completed schematic built in the Express SCH interface, and finished PCB can be seen in figures 37 and 38 respectively.

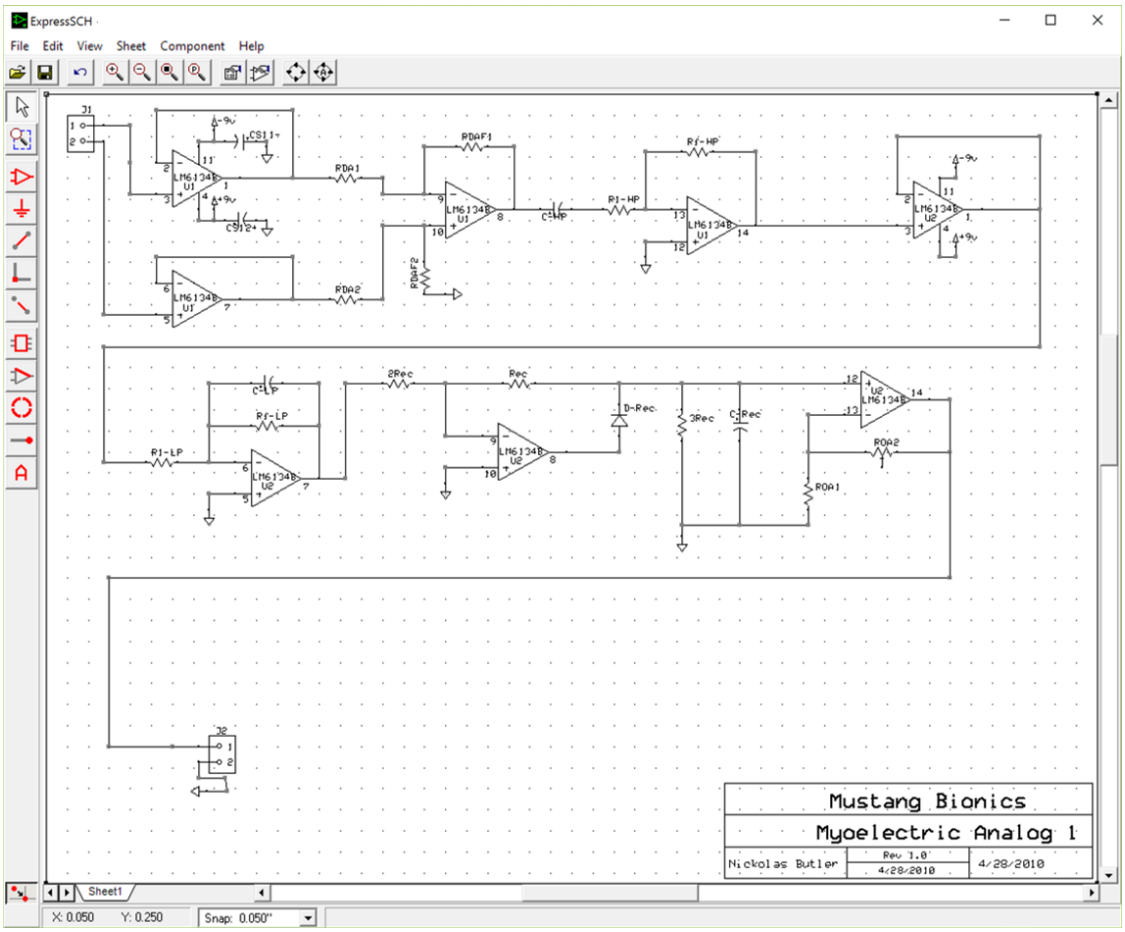

Figure 37: Myoelectric Circuit Unit Constructed in Express SCH software

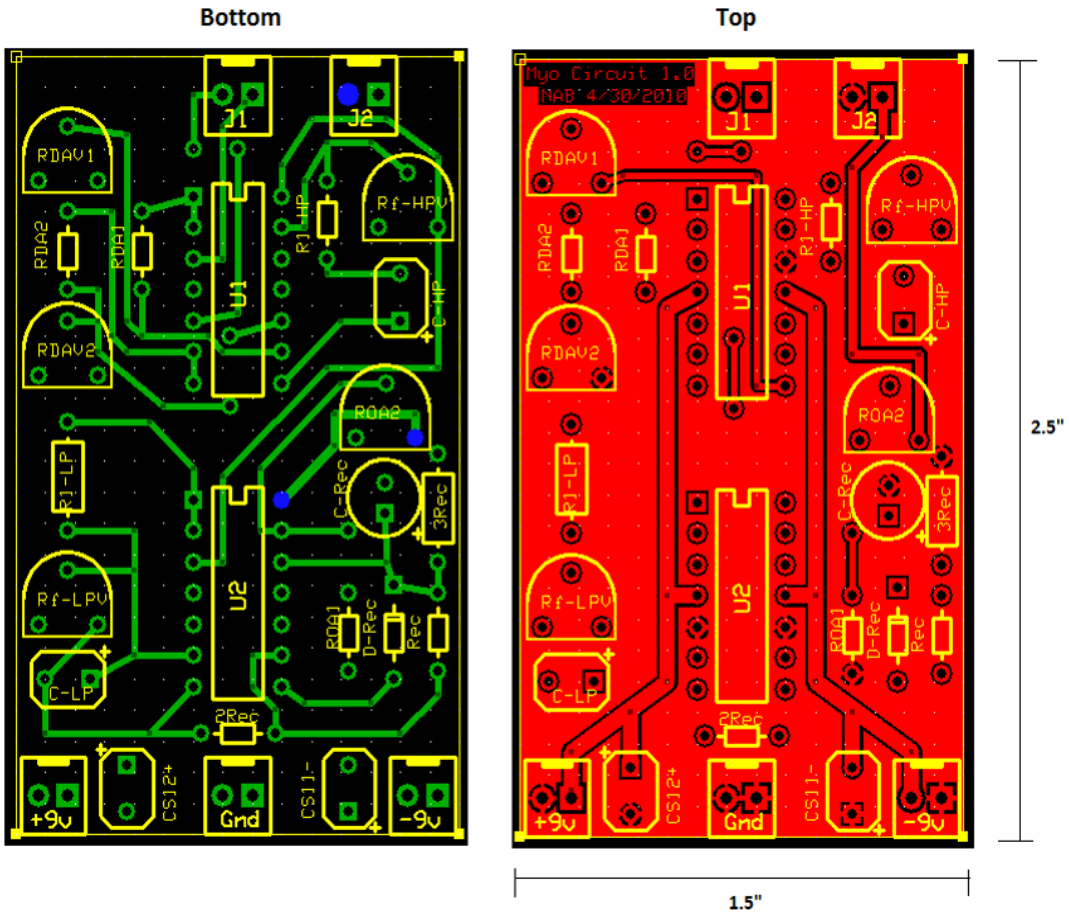

Figure 38: Myoelectric Circuit Unit PCB Layout

To reduce the complexity of the PCB layout, the Texas Instruments LM324A quadruple operational amplifier was used. Two quad op-amps provide enough input and output terminals to construct the eight operational amplifiers present in the circuit. Similar to the LF411, this amplifier has a low supply current of 0.8 mA, good CMRR of 80 dB, and a large gain bandwidth of 100 V/mV [18]. This amplifier can also act in single and dual power modes (for DC and AC respectively), where the V_{CC} and *GND* pins can also function as *V*+ and *V*- inputs. A diagram of the LM324A quad operational amplifier can be seen in figure 39 below.

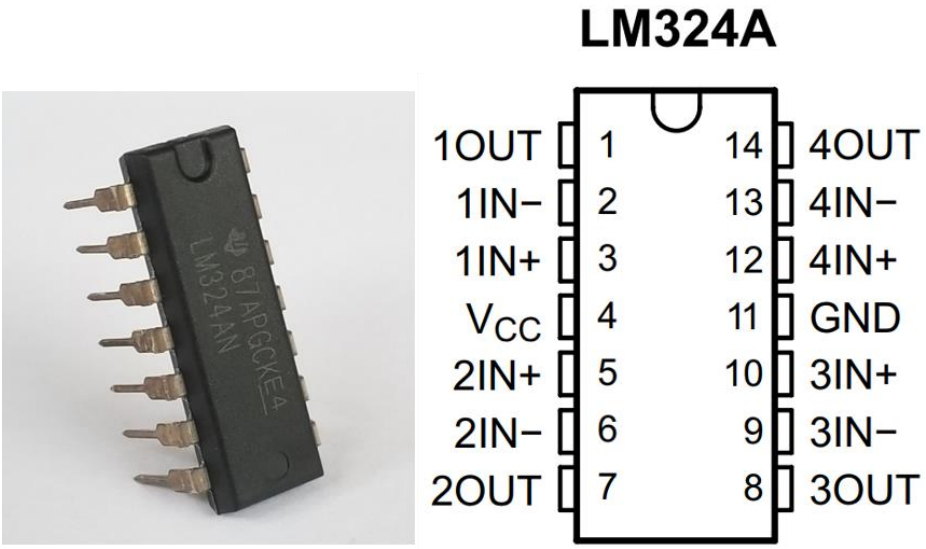

Figure 39: TI LM324AN Quad Op-Amp [18]

3.3.4 PCB Circuit Assembly

After receiving the final dual layer PCB, components were installed according to their respective values and indicated positions. Once fully seated, components were soldered to the PCB, with each connection verified with a multimeter. This verification was performed on all three of the PCB circuits that were received.

For individual gain tuning of each circuit element, 0-10k Ω potentiometers were used, and for power supply spike smoothing, two 10 µF capacitors were connected in parallel with the positive and negative supply voltages. For all of the supply, input, and output terminals, quick connect male terminals were installed. Table V lists the components installed at each terminal of the myoelectric circuit unit. For the complete bill of materials, including component source, refer to section A of the appendix. The fully assembled myoelectric circuit unit can be seen in figure 40 below.

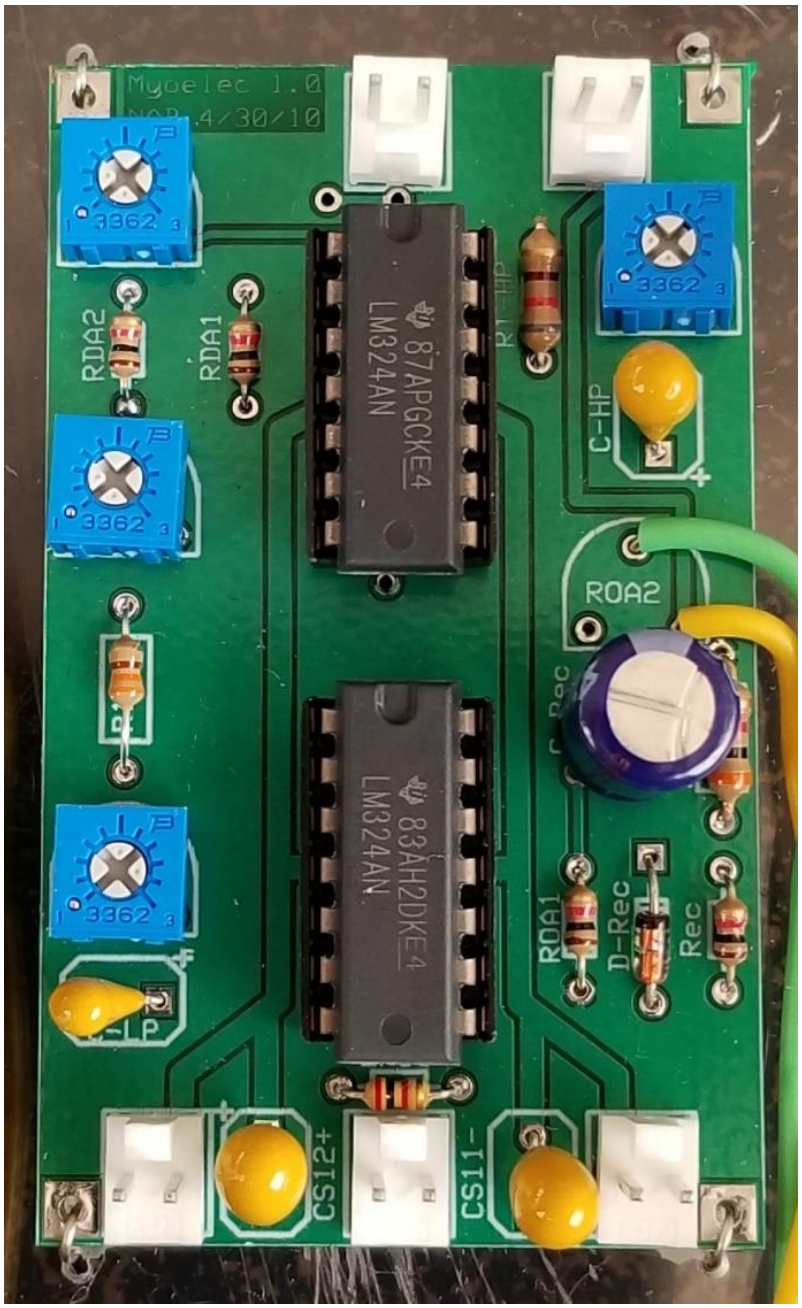

Figure 40: Fully Assembled Myoelectric Circuit Unit PCB

Table V: List of components for Myoelectric Circuit Unit

Name(s)	Type	Units
R1-LP	330	**Ω**
R1-HP	820	**Ω**
RDA1, RDA2, Rec, ROA1	1	**kΩ**
2Rec	2	**kΩ**
3Rec	3	**kΩ**
RDAY1, RDAY2, Rf-HP, Rf-LP, ROA2	0-10 Potentiometer	**kΩ**
C-LP	0.1	**µF**
C-HP, CS11-, CS12+	10	**µF**
C-Rec	470	**µF**
DRec	N1 Zener Diode	N/A
U1, U2	TI LM324AN quad op-amp	N/A
+9V, -9V, Gnd, J1, J2	Molex 2-Pin Male Connector	N/A

3.3.5 Solderless Breadboard Circuit

Once all components were installed and soldered on the three myoelectric circuit unit PCBs, a fourth myoelectric circuit unit was constructed using a small solderless breadboard. This circuit was built using the same components as the PCB version, with additional wiring to bridge component connections. As with the PCB circuits, continuity was verified for all wiring connections, and capacitor and diode polarity were confirmed using a multimeter.

3.4.1 EMG Interface Device Assembly

This section details the design and assembly of additional circuit components, EMG measurement wiring, and the EMG interface device enclosure.

3.4.2 Power Bridge Circuit

To provide power to each of the myoelectric circuit units, a bridge circuit was created on a solderless breadboard. This circuit relays power from both the Arduino Leonardo's 5V USB supply terminal (connects to (+) positive input), and a 9V battery (connects to (-) negative input) to all eight of the myoelectric circuit unit LM324AN op-amps. Also, the positive power source could be switched to run from a 2nd 9V battery instead of Arduino power if desired. In addition to power management, this circuit also supplied the input terminal for the electrode ground, and branched the connection to each of the four myoelectric circuit units. The layout of this circuit is shown in section 3.4.5 below.

3.4.3 EMG Measurement Wiring

Four dual-connector wires were constructed for each of the myoelectric circuit units. Each wire bundle was approximately 3' in length, and had two button connectors that easily snap onto standard EMG/ECG surface electrodes. Polystyrene heat heat-shrink was placed over the wires for easier handling, and protection. Finally, metal connector crimps were attached to the end of each exposed wire, and a dual slot female connection terminal was installed. A fully assembled EMG measurement wire can be seen in figure 41 below.

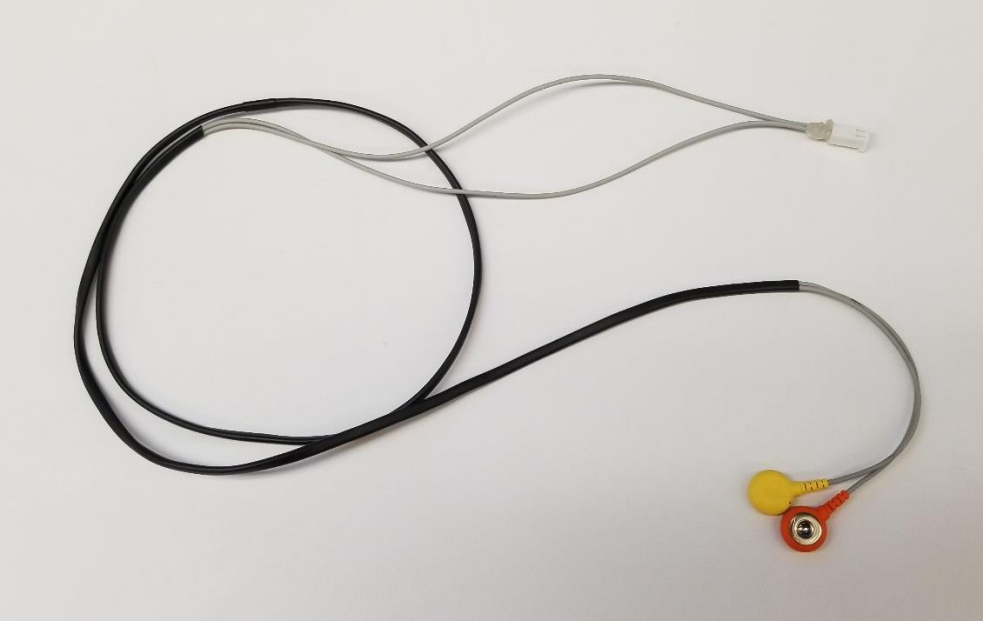

Figure 41: EMG Measurement Wire Bundle

3.4.4 Device Enclosure and Mounting

Once all four of the myoelectric circuit units were constructed, they were arranged in a transparent plastic enclosure, measuring 11” x 6.5” x 2”. For permanent mounting, 1/16” holes were drilled in pairs at the four corners of each PCB, and 40-gauge wire was routed through the holes in the PCB and the enclosure, and finally twisted to secure. Both solderless breadboard circuits were mounted to the enclosure through an adhesive backing.

Next, the Arduino Leonardo microcontroller and 9V battery power sockets were arranged in the enclosure. Both of these components were installed and mounted by drilling two 1/8” diameter holes in the enclosure, and fastened with two plastic 4-40 socked head cap screws and #4 hex nuts.

For each of the myoelectric circuit units, breakout wiring was soldered to the final amplifier terminal, *ROA2*. Dial potentiometers operating at 0-10 kΩ were attached to this breakout wiring, to provide an easy-to-use interface for final amplifier gain tuning. Appropriately sized holes were drilled in the front wall of the enclosure, and the potentiometers were installed through the holes and fastened.

To allow for all wiring to pass through the enclosure, holes were also drilled for the microcontroller USB cable, four EMG inputs, and grounding electrode. Finally, access holes were drilled for two mounted power switches.

3.4.5 EMG Interface Device Summary

The EMG interface device, comprised of four Myoelectric Circuit Units, an Arduino Leonardo microcontroller, battery terminals, a power bridge circuit, and EMG electrode wiring, was connected and assembled inside of a transparent enclosure. A detailed diagram of the device can be seen in figure 42 below, with additional pictures available in section B of the appendix.

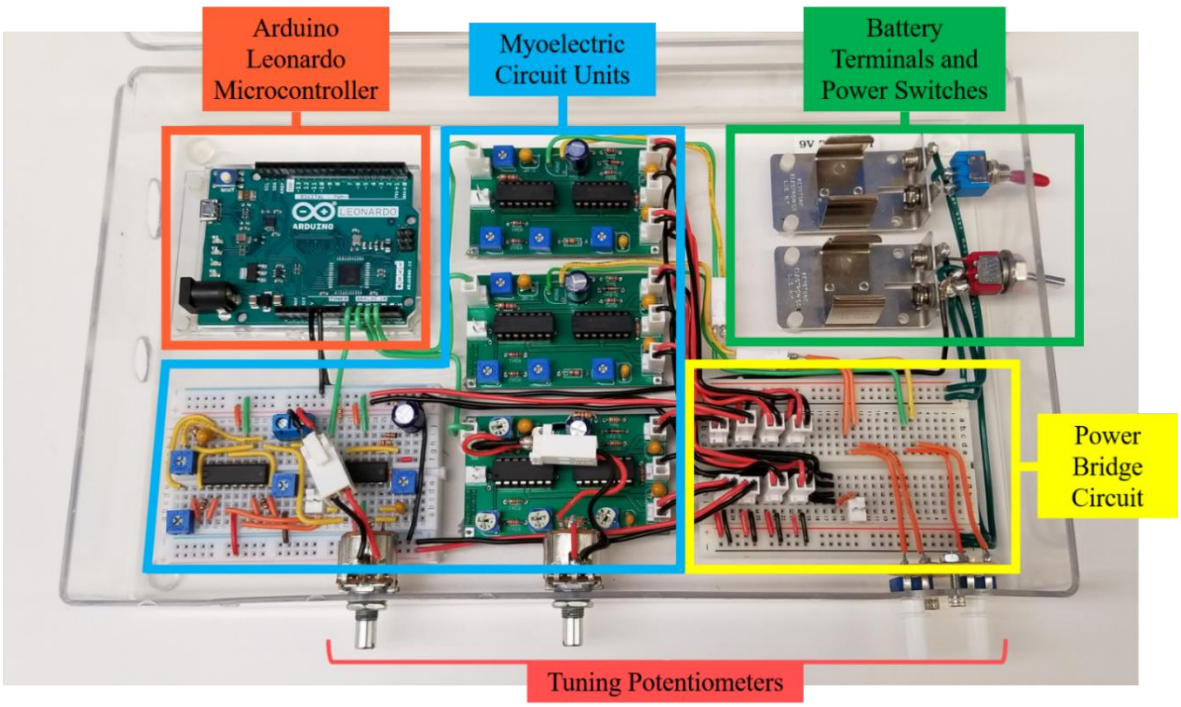

Figure 42: The EMG Interface Device

3.5.1 Arduino Leonardo Software

To achieve the desired software specifications presented in chapter 2, a sketch was created in the Arduino software interface. This sketch allowed for an analog signal to be read and converted to a digital Boolean value. As multiple EMG values were read in, a calibration routine allowed for the device user to specify the threshold at which mouse cursor movement would begin. Next, when a measured EMG signal value exceeded the activation threshold, the software would command the connected PC to move the mouse cursor in the specified direction via a serial USB connection. Also, mouse cursor speed could be controlled by the intensity of the generated EMG signal, and a mouse "left click" was simulated when multiple inputs were activated simultaneously.

3.5.2 Software Review

The software sketch that was installed on the Arduino Leonardo microcontroller as part of the EMG interface device, was comprised of 116 lines of code written in the Arduino programming language. Debugging was carried out both through the Arduino interface serial monitor, where inputs could be sent and values displayed, and through physical testing of the EMG interface device, where generated signals would move a PC mouse cursor.

The first step in the sketch was to initialize the mouse cursor movement library, where the appropriate hardware driver would be installed on the microcontroller. Next, many different variables were declared, such as analog pin numbers for the four EMG inputs, activation thresholds from which cursor movement would begin, and various logic flags, cursor movement variables, and EMG scaling factors. After all declarations had been made, the setup code for the program would commence, where the serial USB connection would be established, and the mouse movement routine would be activated.

Next came the main loop of the program, where first the EMG threshold calibration routine would start. This routine would alternate between providing written instruction via the serial monitor, reading the incident EMG signal, and calculating the activation threshold at which mouse cursor movement would begin. First the user would be instructed to flex their muscle corresponding to one cursor movement direction and hold for several seconds. Next, a looping routine would collect many readings from an analog input corresponding to the direction specified, and sum the readings into one integer variable. This variable would then be divided by the number of readings to calculate the average value. This value would then be multiplied by a scaling factor, and

used to define the EMG activation threshold for mouse cursor movement. After calibrating the activation threshold for one input direction, the routine would then proceed to instruct, measure, and calculate the threshold for the other three inputs.

Once all calibration steps were complete, the program would then transition to the mouse cursor movement routine. This routine relied on a series of logic conditions where the current measured analog EMG input would be compared to the previously established activation threshold. As soon as one of the logic conditions was found to be true, the mouse cursor would be instructed to move in the specified direction a set number of pixels. Next, a software delay routine would be initiated, where the proportional value of the EMG reading relative to the activation threshold would decrease the delay time specified. The purpose of this delay routine was to give the user direct control over the speed of the cursor. This would be achieved through intentional flexing of the target muscle, which would increase motor unit recruitment and magnitude of the generated EMG signal.

At the end of the program, a routine was created that allowed for a mouse “left click” button to be controlled. This was carried out through a dual-conditional logic statement, which evaluated two of the four measured EMG inputs. When the device user intentionally flexed two of the measured inputs forcefully, which could be achieved by forming a fist, the program would register this event and command the mouse to “left click”. For the complete Arduino sketch code, with comments included, refer to section C of the appendix.

In summary, a software program was written in the Arduino language that was loaded onto the Arduino Leonardo microcontroller. Contained in this program was the

necessary library files to establish a USB connection with a PC and simulate mouse hardware drivers. Once this connection had been made, the program allowed for the user to calibrate the EMG interface device to their specific measurement thresholds. After establishing these thresholds, the program would monitor four discrete analog inputs, where EMG signals captured by the myoelectric circuit units would be read in. As soon as these inputs read above the calibration settings, the program would command the mouse cursor to move in the user's desired direction.

3.6.1 Test Methods

The following section details the methods applied to conduct two tests related to the EMG interface device. The first test conducted involved measurement of the current draw, in an effort to estimate the available device use time. Finally, the performance and efficacy of the device was evaluated through a human model test, which involved typing on an on-screen PC keyboard by moving a cursor with the device.

3.6.2 Device Current Draw Test

For each of the iterations of the myoelectric circuit units (solderless breadboard, soldered protoboard, and PCB), a current draw test was conducted to evaluate device battery consumption. Two digital multimeters were used, and set to current measuring mode in milliamps. Current was measured by connecting a multimeter in series for both the positive and negative power supplies. Data was recorded when the circuit was in the "on" state, but idle, as well as the maximum EMG signal amplification state. Total current was determined by adding the measurements from both connection multimeters.

Once the test had been completed on each iteration of the myoelectric circuit unit, the test was repeated for the entire EMG interface device. This time, current was measured for the negative 9 V battery power supply, and the positive 5 V supply from the Arduino microcontroller. The data collected for both of these tests is presented in the results section of the next chapter.

3.6.3 Device Efficacy in Human Model Test

To evaluate performance of the EMG interface device, a test was created in which the device user would perform a series of instructions while being timed. The purpose of this test was to quantify the efficacy of the device, where the accuracy and speed could be measured and compared to a control.

To perform the test, the device user was instructed to type out the full alphabet using an on-screen keyboard, by moving the mouse cursor to select the letter, and "left clicking" on the key to type. While this test was performed, the user's time to completion was measured. Also, if the user mistakenly missed or clicked on an un-desired letter, they were asked to move on to the next letter. This was done to evaluate the device accuracy and general ease of use.

First, to establish a control, the user was asked to type out the full alphabet three times using a standard PC mouse. Next, the user was instructed to perform the same test three times using the EMG interface device with electrodes only connected to the forearm, and ground reference. The muscles in the forearm that were target were the flexor carpi ulnaris and radialis, as well as the extensor carpi ulnaris and radialis longus. An example of the electrode placement used for this test can be seen in figure 43 below.

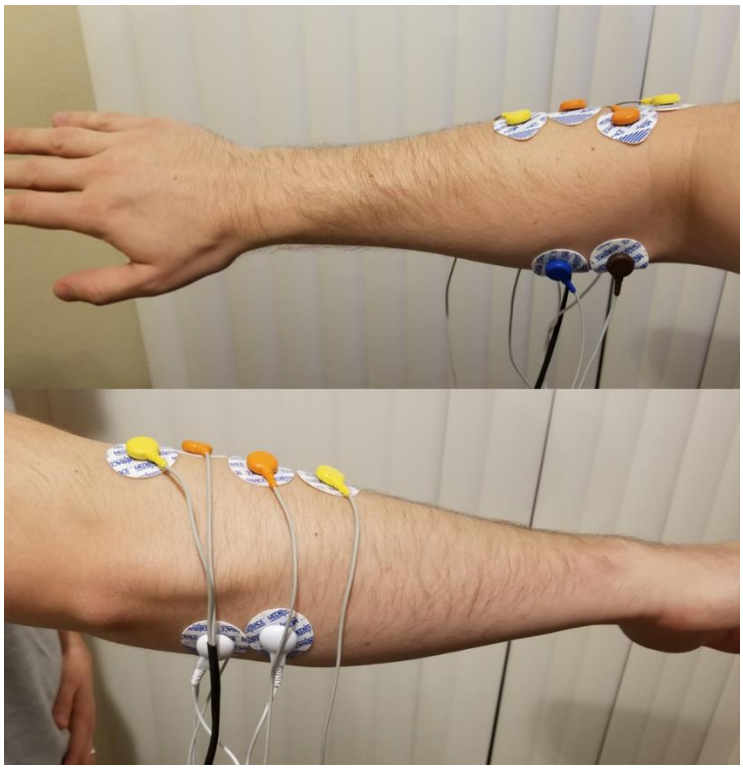

Figure 43: Electrode placement on forearm

Finally, the test was repeated with two pairs of electrodes placed over the flexor carpi radialis and extensor carpi ulnaris muscles on the forearm (for cursor move left and right), and two pairs connected to the user's biceps brachii and triceps brachii muscles (for cursor move up and down). Different from the previous test, cursor movement up and down would be controlled by elbow flexion and extension, instead of wrist deviation. The electrode placement used in this test can be observed in figure 44 below.

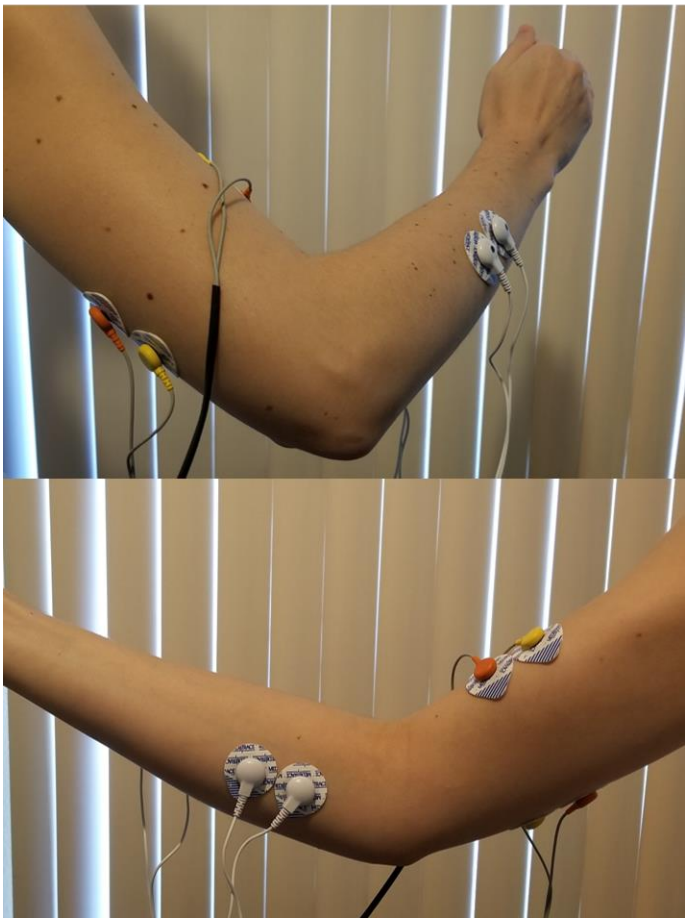

Figure 44: Electrode placement on forearm and upper arm

To provide more comfort when performing mouse “left click”, a foam stress ball was held in the user’s hand and squeezed to activate the forearm muscles simultaneously. Two device users were tested for all three tests. The results of these tests can be seen in chapter 4.

Chapter 4

RESULTS

In this chapter, data collected for two tests is presented; EMG interface device power draw, and device efficacy in human model test.

4.1.1 EMG Interface Device Current Draw Results

The results of the myoelectric circuit unit current draw test can be observed in figure 45 below. Data was collected for the three iterations of the circuit; the solderless breadboard prototype, the soldered protoboard, and the final through-pin (DIP) masked PCB circuit. Current was measured in milliamps (mA) for each circuit, both in an idle state and maximum EMG signal amplification resulting from muscle flexion.

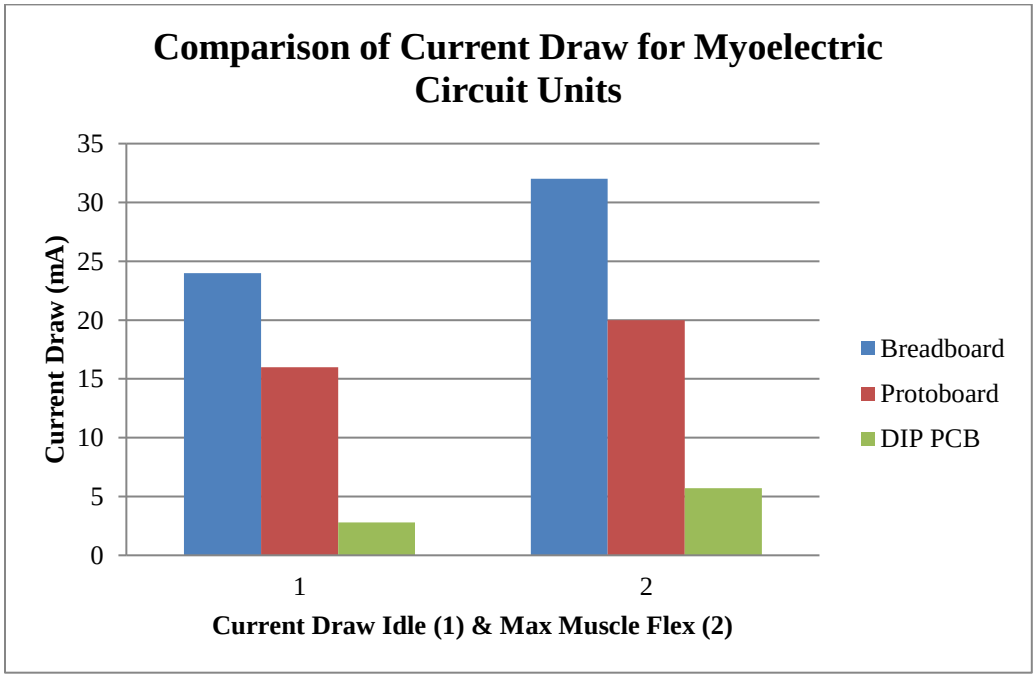

Figure 45: Results from myoelectric circuit unit current draw test

For the entire EMG interface device (EID), total current draw was measured for both the idle and max EMG flex states. The results of this test can be seen in figure 46 below.

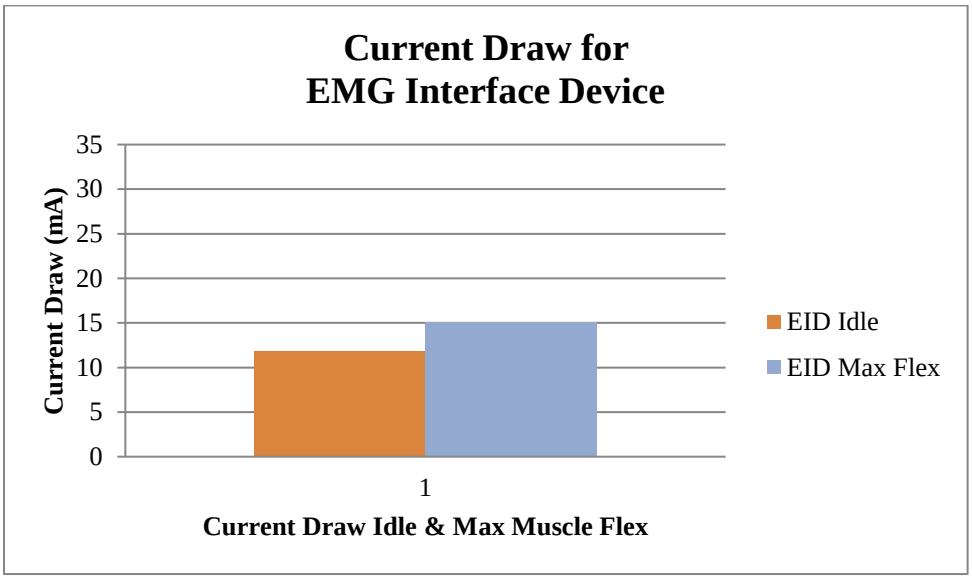

Figure 46: Results from EMG Interface Device current draw test

4.1.2 Device Efficacy in Human Model Test Results

The results of the device efficacy human model test can be found in table VI below. Data was collected from two device users, one male of average build and one female of slender build, both age 32. This table specifies the device user, test type performed, test number, individual test time, average test time, individual test accuracy, average test accuracy, and generated keystrokes. Accuracy was determined by evaluating the entered keystrokes relative to the standard 26 letter alphabet. An incorrect letter entry or duplicate entry was counted as 1/26 wrong. Average accuracy was calculated from the results of the 3 tests.

Table VII: Device Efficacy Results

User	Test Type	Test	Time (min)	Average (min)	Accuracy	Average (%)	Keystrokes
Male 32 y/o	PC Mouse (Control)	1	0:27	0:24	26/26	100%	Abcdefghijklmnopqrstuvwxyz
		2	0:22		26/26		Abcdefghijklmnopqrstuvwxyz
		3	0:22		26/26		Abcdefghijklmnopqrstuvwxyz
	EID: Forearm	1	2:41	2:11	26/26	99%	Abcdefghijklmnopqrstuvwxyz
		2	2:00		26/26		Abcdefghijklmnopqrstuvwxyz
		3	1:54		25/26		Abcdefghijklmnopqrdstuvwxyz
	EID: Forearm + Upper arm	1	1:45	1:36	24/26	91%	Abcdefghijklmnopqrstuvrqwxyz
		2	1:33		23/26		Abcdefghihjklmniopqrstuvewxyz
		3	1:31		24/26		Abcdefghuijklmnopqrstuvwcxyz
Female 32 y/o	PC Mouse (Control)	1	0:26	0:22	26/26	100%	Abcdefghijklmnopqrstuvwxyz
		2	0:21		26/26		Abcdefghijklmnopqrstuvwxyz
		3	0:19		26/26		Abcdefghijklmnopqrstuvwxyz
	EID: Forearm	1	3:11	2:42	25/26	87%	Abcdefghijklmniopqrstuvwxyz
		2	2:09		24/26		Abcdefghijklmnopqerstyuvwxyz
		3	2:47		22/26		Qabcdefghijklmnopqrewstucvwxyz
	EID: Forearm + Upper Arm	1	2:55	2:19	19/26	82%	Abcdefghuijjklmnoopqqerastyuvwxyz
		2	2:14		22/26		Avbbcdefghijklmbnopqrqstuvwxyz
		3	1:48		23/26		Aabcdefghijklmnopqrzstuvqwxyz

Chapter 5

DISCUSSION AND CONCLUSIONS

5.1.1 Discussion of Current Draw Test Results

Evaluating the results from the current draw test for the myoelectric circuit unit, it can be observed that a clear power efficiently improvement was gained through each subsequent design iteration. From the initial breadboard prototype, to the final DIP PCB, an 88.3% power efficiency improvement was gained for the idle state, and an 82.3% improvement for max amplification. This substantial current draw improvement is likely attributed to shorter wiring/trace paths, fewer components, and primarily, the change from individual LF411 op-amps, to the LM324A quad op-amp.

For the EMG interface device current draw test, results showed a maximum current draw for the idle state of 11.8 mA, and 15.1 mA for max amplification. This measurement reflected the total current draw from both the positive Arduino supply, and the negative supply from a 9V battery. Since the Arduino supply is powered by PC USB, the limiting factor for device use time would be the 9V battery supply. Assuming a 50% duty cycle between the idle and max current draw states, 50% of the power drawn from the negative supply, and a 600 mA-hours life for an Energizer 9V battery, the following calculation was made to determine the device use time [19].

$$Device\ Use\ Time = \frac{600\ mAHours}{\left(\frac{11.8\ mA + 15.1\ mA}{4}\right)} = 44.6\ Hours$$

5.1.2 Discussion of Device Efficacy Human Model Test Results

Upon reviewing the results from the device efficacy human model test, it was observed that the device efficacy relative to the standard PC mouse control was less in both metrics. For the fastest time to complete electrode configuration, “forearm + upper arm”, the average time relative to the mouse control was found to be significantly slower, with over a minute slower for the male user, and nearly two minutes slower for the female user. The accuracy of alphabet entry was also found to be less relative to the mouse control, but the “forearm” tests for the male subject were found to be close to mouse control, with an entry accuracy of 99%.

Comparing the EMG interface device tests performed, it was observed that the “forearm + upper arm” electrode configuration completed the test significantly faster in all tests performed, with the male user finishing 35 seconds faster, and the female user finishing 23 seconds faster on average. For entry accuracy however, the “forearm” test was observed to be most accurate across all tests performed, with the male user gaining 8% greater entry accuracy, and the female user gaining 5% accuracy on average.

For all tests with the EMG interface device, with one exception, the time to complete the test continued to drop with each subsequent test performed, with the female user seeing over a minute decrease in time for the “forearm + upper arm” configuration. This progressive time drop suggests that the user was learning to use the device more efficiently, and better identify the specific wrist and arm motions that produced the desired result. With more practice, perhaps even better completion time could be achieved.

After running each test, comments and feedback was gathered from the user. The most prominent feedback that was given was that the “forearm + upper arm” electrode configuration was significantly more comfortable and easier to control, relative to the “forearm” configuration. It was stated that that “cursor up” and “cursor down” commands were very difficult to distinguish, and would often move “cursor left” and “cursor right” as well. Also, these two cursor directions were activated by radial and ulnar deviations (wrist side to side), which have a very short range of motion, and were found to cause discomfort in some cases. This feedback was not surprising, as the superficial muscles in the forearm reside very close to each other, and present a challenge for surface electrodes to easily distinguish. For some of the “forearm” test cases, electrode placement had to be redone and the software re-calibrated several times to even achieve usable cursor control. This was contrasted by the “forearm + upper arm” tests, where electrodes were easily placed evenly on large independent muscle groups, and cursor control was achieved about primary flexion and extension fulcrums (wrist and elbow). These results corroborate the study conducted by Jin Lee et al, which highlighted the importance and effect of selective electrode placement for EMG signal capture [5]. Other feedback provided was that the EMG measurement wires frequently got in the way of cursor move motions, and that ability to move the cursor diagonally, and not purely in X and Y coordinates was highly desired.

When asked whether the user was aware of the ability to control cursor velocity, both users agreed that they could, but that this feature was more discernable and useful in the “forearm + upper arm” tests. It was stated that the smoother cursor movement of this test allowed the cursor velocity increase to be intentionally activated and held, relative to

the “forearm” test, where the cursor frequently moved in undesired directions. This feedback highlights the study conducted by Liping Qi et al, where the force generated by the user’s movement directly correlates to EMG signal amplitude and, in this case, is harnessed for dynamic cursor velocity control [4].

As presented with these results, the EMG interface device efficacy test highlighted how meaningful mouse cursor control and PC interaction could be achieved through voluntary EMG signal activation. While these tests were carried out by non-disabled individuals, the results of this test suggest that the device could be of use to those who cannot use a standard PC mouse, and remaining voluntary muscle groups are targeted. For non-disabled individuals, this device did not show any improved effectiveness over a standard PC mouse. With the ability to place electrodes on any superficial muscle group in the body however, novel uses may exist, where additional input degrees are desired.

5.1.3 Challenges Faced

Over the course of this thesis project, several significant challenges were faced. The first real challenge arose when the myoelectric circuit unit was first being developed. An early iteration of this circuit, which was designed as part of an electromechanical prosthetic hand project for the Cal Poly QL+ lab, did not employ a differential amplifier circuit, or a properly tuned band-pass filter. This led to significant challenges in isolating a clean and effective EMG signal at the target muscle, due to significant electrical interference from lights, devices, and other sources. The electromechanical prosthetic hand that was connected to this circuit, would jitter significantly, and could not perform desired tasks effectively. Eventually an analog tiered comparator circuit was designed,

that would allow the input signal to fluctuate between four thresholds. Once this threshold has been exceeded, a more stable discrete DC signal would be output. Only after discovering the real necessity of a high input impedance differential amplifier in EMG measurement applications, as described in the study by J. Rosell et al, and by learning to properly manipulate the parameters of the band-pass filter, a cleaner and more usable EMG signal was isolated [7].

Another challenge faced related to the proper placement of surface electrodes over the target superficial muscle. As was demonstrated in the device efficacy test results, inconsistent electrode placement resulted in undesired cursor movement, and significantly more time to complete the test. This problem was ultimately somewhat alleviated by later targeting only large, independent muscle groups in the forearm and upper arm, but originally the inconsistent performance of the EMG interface device led to an effort to create an Arduino algorithm to improve cursor movement. After learning of the study conducted by Yi-Hung Liu et al, where an EMG pattern recognition system using four surface electrodes was developed for mechanical hand movement, a similar signal recognition system was attempted [10]. During the initial calibration routine, this software algorithm measured the signal across all four EMG inputs, saved this signal pattern, and attempted to establish mouse cursor movement through a four-tiered state machine. Unfortunately, the pattern recognition technique used was found to be inconsistent in establishing and recognizing EMG patterns. During this time, there also appeared to be a signal amplification drift what occurred for an unknown reason, which may have affected the recognition technique. Ultimately this recognition technique was

unsuccessful, and was eventually replaced with a discrete input recognition method for each cursor control direction.

When this thesis project was originally conceived, it was planned to combine and miniaturize the four myoelectric circuit units into a single PCB using small surface-mount components. Also, an integrated arm-band was conceptualized, that would possess four sets of discrete metal EMG electrodes, and allow for easier installation and use of the interface device. Eventually both of these plans were set aside once the significant effort of this project was realized.

5.1.4 Improvements and Future Work

As highlighted in the previous section, there were several planned device elements that would likely present significant improvements to the effectiveness and ease of use. For future development of this EMG interface device, significant usability improvements could be gained through an improved method of identifying the user's desired cursor movement. This could be achieved through a surface electrode array with additional inputs, or as previously shown by Yi-Hung Liu et al, a pattern recognition technique [10]. This would likely be the first area of investigation for future improvements.

Another likely improvement to the device would be to integrate all of the analog circuit elements and a microprocessor into one discrete PCB. This would likely further lower power consumption, reduce interference from other electronic sources, and miniaturize the device, such that it could be either combined with a custom electrode arm band, or discretely worn by the user.

An additional avenue for improvement would be to investigate techniques of further leveraging the Arduino platform. Since Arduino is open-source, there exists a multitude of custom circuits that are relatively inexpensive. One such custom circuit is the Arduino Wireless SD Shield, which allows for wireless communication with other electronics [20]. Perhaps an EMG measurement system could be created that removes the requirement to be physically tethered to the device with wires and would provide freedom of movement.

5.1.4 Final Conclusions

For user control of a PC mouse cursor, an EMG interface device was designed and built. The device utilized an array of 1.5” X 2.5” myoelectric circuit units, which individually convert a measured EMG input signal from surface skin electrodes to a clean and usable 0-5 V DC output signal. This analog signal was read to an Arduino Leonardo microcontroller, which would process the signal to digital Boolean value, establish activation thresholds, and command mouse cursor movement through a USB connection when the threshold was exceeded. Also, a proportional comparator algorithm was created that utilized EMG signal amplitude to control cursor velocity. The device was housed in a clear plastic enclosure, and also included an independent power supply, on/off switches, tuning dials for each EMG input, and access ports for all electrode wiring. Testing was performed that showed the device had a long battery life of 44.6 hours, and provided an effective means to move a PC mouse cursor, and type entries on an on-screen keyboard.

BIBLIOGRAPHY

[1] J. Webster, Medical Instrumentation: Application and Design, 3rd ed ed., John Wiley & Sons, Inc., 1998.

[2] K. Saladin, Anatomy & Physiology: The Unity of Form and Function, 4th ed ed., McGraw Hill, 2007.

[3] S. Deutsch and A. Deutsch, "Understanding the Nervous System: An Engineering," *IEEE Press,* pp. chapter 1, pages 5-10, 1993.

[4] Q. Liping, "Spectral properties of electromyographic and mechanomyographic signals during isometric ramp and step contractions in biceps brachii," *Journal of Electromyography and Kinesiology,* pp. 128-135, February 2011.

[5] J. A. A. Lee, "A simulation study for a surface EMG sensor that detects distinguishable motor unit action potentials," *Journal of Neuroscience Methods,* vol. 168, no. 1, pp. 54-63, 2008.

[6] S. J. Dorgan and R. B. Reilly, "A model for human skin impedance during surface functional neuromuscular stimulation," *Rehabilitation Engineering,* pp. 341-348, 1999.

[7] J. Rosell and e. al, "Skin impedance from 1 Hz to 1 Mhz," *Biomedical Engineering,* p. 649, August 1988.

[8] J. V. Basmajian and C. J. De Luca, Muscles Alive: their functions revealed by electromyography, 5th ed ed., Baltimore, Maryland: Williams and Wilkins, 1985.

[9] C. J. De Luca, Surface Electromyography: detection and recording, DelSys, Inc., 2002.

[10] Y.-H. Liu and H.-P. Huang, "Towards a high-stability EMG recognition system for prosthesis contro:l a one-class classification based non-target EMG pattern filtering scheme," in *IEEE International Conference on Systems, Man, and Cybernetics,* San Antonio, TX, USA, 2009.

[11] T. Lalitharatne, Y. Hayashi, K. Teramoto and K. Kiguchi, "A Study on Effects of Muscle Fatigue on EMG-Based Control for Human Upper-Limb Power-Assist," *ICIAfS'12,* pp. 124-128, 2012.

[12] S. Siriprayoonsak, *Real-Time Measurement of Prehensile EMG Signals*, San Diego State University, 2005.

[13] "Getting Started | Foundation > Introduction," 2018. [Online]. Available: https://www.arduino.cc/en/guide/introduction.

[14] Arduino, "ARDUINO PRODUCTS > Arduino Leonardo," 2018. [Online]. Available: https://www.arduino.cc/en/Main/Arduino_BoardLeonardo.

[15] N. Hamilton, "The Upper Extremity: The Elbow, Forearm, Wrist, and Hand," in *Kinesiology: Scientific Basis of Human Motion*, McGraw-Hill Education, 2011.

[16] "The Muscles of the Arm and Hand," 2015. [Online]. Available: https://anatomy-medicine.com/musculoskeletal-system/87-the-muscles-of-the-arm-and-hand.html.

[17] Texas Instruments Incorporated, "LF411 Precision JFET-input Operational Amplifier," 2018. [Online]. Available: http://www.ti.com/product/LF411.

[18] Texas Instruments Incorporated, "LM324A Quadruple Operational Amplifier," 2018. [Online]. Available: http://www.ti.com/product/LM324A/technicaldocuments.

[19] "Energizer 6LR61 Product Datasheet," 2018. [Online]. Available: http://data.energizer.com/pdfs/alk-power-9v.pdf.

[20] "Arduino Wireless SD Shield," 2018. [Online]. Available: https://store.arduino.cc/usa/arduino-wirelss-sd-shield.

[21] C. P. Fermo and e. al, "Development of an adaptive framework for the control of upper limb myoelectric prosthesis," *Engineering in Medicine and Biology Society*, 2000.

[22] B. D. Farnsworth and e. al, "Wireless In Vivo EMG Sensor for Inteligent Prosthetic Control," in *Solid-State Sensors, Actuators and Microsystems Conference*, 2009.

[23] Y. Wonkeun and K. Jung, "Development of a Compact-size and Wireless Surface EMG Measurement System," *ICCAS-SICE*, 2009.

APPENDICES

A. EMG Interface Device Bill of Materials

Description	Value	Total Device Qty.	Source
Resistor	330 Ω	4	https://www.digikey.com/short/j1jqqh
Resistor	820 Ω	4	https://www.digikey.com/short/j1jqqb
Resistor	1 kΩ	16	https://www.digikey.com/short/j1jtw3
Resistor	2 kΩ	4	https://www.digikey.com/short/j1jqqd
Resistor	3 kΩ	4	https://www.digikey.com/short/j1jq8t
Trimmer Potentiometer	0-10 kΩ	16	https://www.digikey.com/short/j1jq8h
Dial Linear Potentiometer	0-10 kΩ	4	https://www.digikey.com/short/j1jqrn
Capacitor	0.1 µF	4	https://www.digikey.com/short/j1jqf9
Capacitor	10 µF	12	https://www.digikey.com/short/j1jq2z
Capacitor	470 µF	4	https://www.digikey.com/short/j1jqzn
N1 Zener Diode	N/A	4	https://www.digikey.com/short/j1jq20
TI LM324AN quad op-amp	N/A	8	https://www.digikey.com/short/j1jqmt
Molex 2-Pin Male Connector	N/A	29	https://www.digikey.com/short/j1jqmq
Molex 2-Pin Female Connector	N/A	29	https://www.digikey.com/short/j1jqm9
Molex Female Terminal Crimp	N/A	60	https://www.digikey.com/short/j1jqhm
On/Off Toggle Switch	5 Amps	2	https://www.digikey.com/short/j1j87c
Solderless Breadboard	3.2" X 2.0"	2 (or 1)	https://www.digikey.com/short/j1jqh0
Myoelectric Custom PCB	1.5" X 2.5"	3 (or 4)	https://www.expresspcb.com/
Arduino Leonardo Microcontroller	N/A	1	https://store.arduino.cc/usa/arduino-leonardo-with-headers
Jumper Wire Assortment Kit	22 AWG	1	https://www.digikey.com/short/j1jqdh
Shielded EMG Jumper Wires	N/A	9	Pack of 3 wires: http://a.co/d/e67cexf
Adhesive Surface Electrodes	N/A	9	Pack of 100: http://a.co/d/4TW4U0s
9V Battery Holder	N/A	2	https://www.mcmaster.com/7712k62
Plastic Project Box	11" X 7" X 2"	1	https://www.mcmaster.com/4629t53
Plastic Socket Head Screw	4-40	4	https://www.mcmaster.com/95868a256
Plastic Hex Nut	4-40	4	https://www.mcmaster.com/90059a005
Bendable Mounting Wire	OD: 0.025"	1	https://www.mcmaster.com/8860k13
Battery	9 Volt	1	http://a.co/d/9Ad2xDd

B. EMG Interface Device Reference Images

EMG Interface Device wiring layout

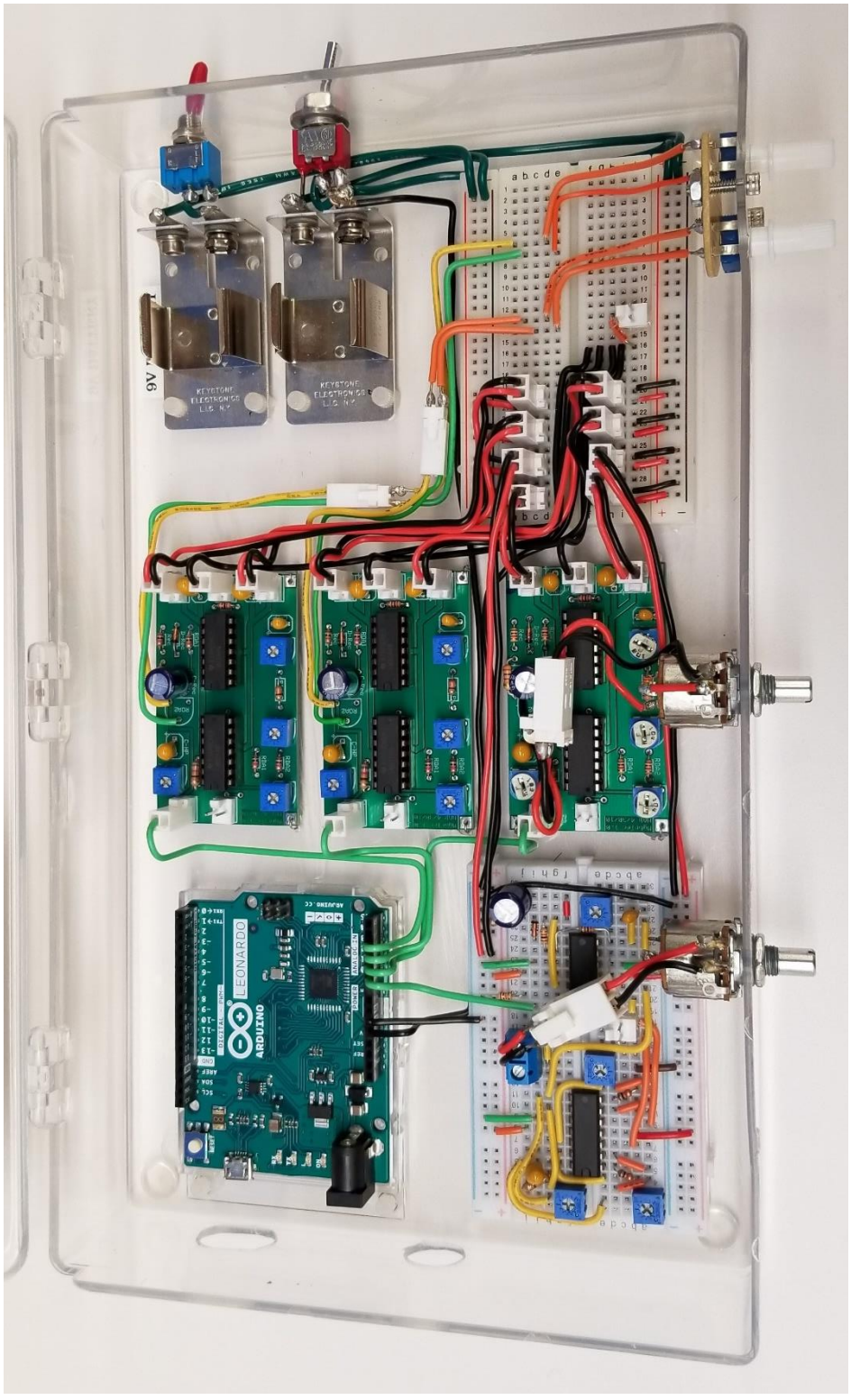

EMG Interface Device with labels

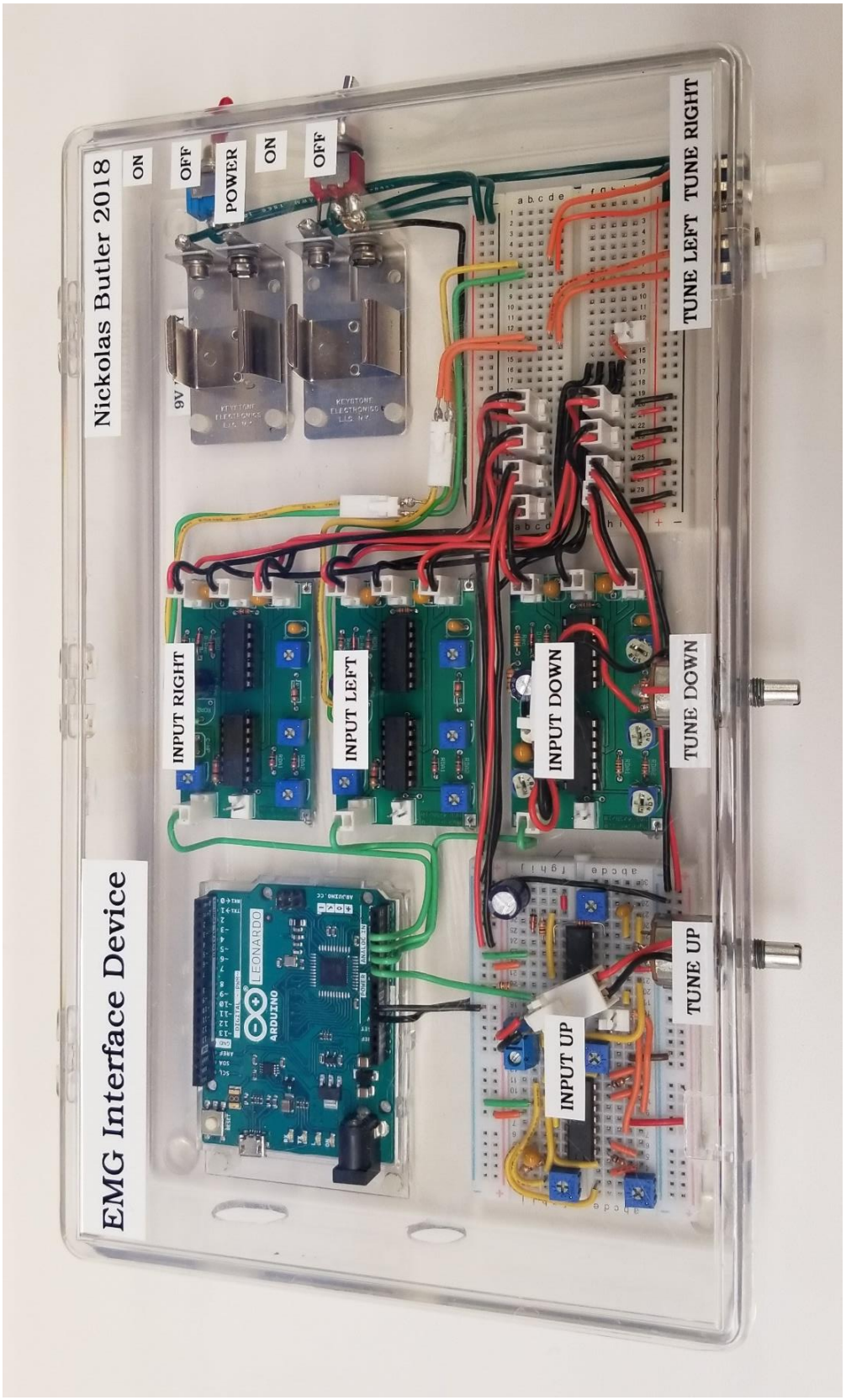

C. EMG Interface Device Arduino Sketch Code

```
// EMG Interface Device Thesis Code
// Cal Poly San Luis Obispo
// Nickolas Butler 2018

// Initialize library
#include "Mouse.h"

// Assign pin numbers for 4 EMG inputs
int myoPinUp = 0;
int myoPinDown = 1;
int myoPinLeft = 2;
int myoPinRight = 3;

// Initialize EMG Activation Thresholds
long myoLimitUp = 0;
long myoLimitDown = 0;
long myoLimitLeft = 0;
long myoLimitRight = 0;

// Initialize Variables
int stateVar = 0;          // Flag designating code to run in main loop
int printVar = 0;          // Flag designating message to display in
main loop
char entryVar = '0';       // Variable for entry selection
int delayTime = 20;        // Initial delay time
unsigned int velDelta = 0; // Calculated delay time
int delayClick = 800;      // Mouse click debounce in milliseconds
int pixelStep = 5;         // Number of pixels on screen cursor moves
per activation
float myoScale = 0.9;      // Activation Threshold Offset
float velScale = 1.1;      // Multiplication factor for cursor velocity
control (Larger value = faster cursor)


// Initialization Code
void setup()
{
  Serial.begin(9600); // Start USB Serial Connection
  delay(3000);

  // Start mouse control
  Mouse.begin();
}

// Main Loop
void loop()
{
  if (stateVar == 0)
  {
    // EMG Calibration Instructions
```

```
    // Check printVar for text to display
    if (printVar == 0)
    {
      Serial.println("EMG Interface Device");
      Serial.println("Cal Poly San Luis Obispo");
      Serial.println("Nickolas Butler 2018");
      Serial.println("Signal Calibration Routine");
      Serial.println("Flex muscle in direction for Up and hold for 5
seconds.");
      Serial.println("When ready, enter 1 and press Enter.");
      printVar = 1;
    }
    else if (printVar == 2)
    {
      Serial.println("Flex muscle in direction for Down and hold for 5
seconds.");
      Serial.println("When ready, enter 2 and press Enter.");
      printVar = 3;
    }
    else if (printVar == 4)
    {
      Serial.println("Flex muscle in direction for Left and hold for 5
seconds.");
      Serial.println("When ready, enter 3 and press Enter.");
      printVar = 5;
    }
    else if (printVar == 6)
    {
      Serial.println("Flex muscle in direction for Right and hold for 5
seconds.");
      Serial.println("When ready, enter 4 and press Enter.");
      printVar = 7;
    }

    // Calibrade EMG threshold for 4 inputs
    // Check entryVar for input to calibrate
    if (Serial.available() > 0)
    {
      entryVar = Serial.read();
      if (entryVar == '1')
      {
        delay(1000);
        // Averaging Loop
        for (int i = 0; i <= 100; i++)
        {
          delay(30);
          myoLimitUp = myoLimitUp + analogRead(myoPinUp); // Sum 100
EMG Values
        }
        myoLimitUp = (myoLimitUp / 100) * myoScale; // Calculate
average and adjust threshold
        Serial.println("UP threshold set to:");
        Serial.println(myoLimitUp);
        printVar = 2; // Set flag to print next calibration message
```

```
        delay(1000);
      }
      else if (entryVar == '2')
      {
        delay(1000);
        // Averaging Loop
        for (int i = 0; i <= 100; i++)
        {
          delay(30);
          myoLimitDown = myoLimitDown + analogRead(myoPinDown); // Sum
100 EMG Values
        }
        myoLimitDown = (myoLimitDown / 100) * myoScale; // Calculate
average and adjust threshold
        Serial.println("DOWN threshold set to:");
        Serial.println(myoLimitDown);
        printVar = 4; // Set flag to print next calibration message
        delay(1000);
      }
      else if (entryVar == '3')
      {
        delay(1000);
        // Averaging Loop
        for (int i = 0; i <= 100; i++)
        {
          delay(30);
          myoLimitLeft = myoLimitLeft + analogRead(myoPinLeft); // Sum
100 EMG Values
        }
        myoLimitLeft = (myoLimitLeft / 100) * myoScale; // Calculate
average and adjust threshold
        Serial.println("LEFT threshold set to:");
        Serial.println(myoLimitLeft);
        printVar = 6; // Set flag to print next calibration message
        delay(1000);
      }
      else if (entryVar == '4')
      {
        delay(1000);
        // Averaging Loop
        for (int i = 0; i <= 100; i++)
        {
          delay(12);
          myoLimitRight = myoLimitRight + analogRead(myoPinRight); //
Sum 100 EMG Values
        }
        myoLimitRight = (myoLimitRight / 100) * myoScale; // Calculate
average and adjust threshold
        Serial.println("RIGHT threshold set to:");
        Serial.println(myoLimitRight);
        stateVar = 1; // Set flag to exit calibration routine
        delay(1000);
      }
    }
```

```
  }

  // Mouse Cursor Move Code
  // Don't run until calibration routine is complete (check flags)
  if (stateVar == 1 && printVar == 7)
  {
    Serial.println("Mouse control START");
    if (analogRead(myoPinUp) > myoLimitUp)
    {
      Serial.println("UP");
      Serial.println(analogRead(myoPinUp)); // Display EMG value
      Mouse.move(0, -pixelStep); // Move cursor specified increment
      velDelta = (delayTime / ((analogRead(myoPinUp) / myoLimitUp) *
velScale)); // Cursor velocity control: scale movement delay by ratio
of reading over threshold
      delay(velDelta);
    }
    else if (analogRead(myoPinDown) > myoLimitDown)
    {
      Serial.println("Down");
      Serial.println(analogRead(myoPinDown));  // Display EMG value
      Mouse.move(0, pixelStep); // Move cursor specified increment
      velDelta = (delayTime / ((analogRead(myoPinDown) / myoLimitDown)
* velScale)); // Cursor velocity control: scale movement delay by ratio
of reading over threshold
      delay(velDelta);
    }
    else if (analogRead(myoPinLeft) > myoLimitLeft)
    {
      Serial.println("Left");
      Serial.println(analogRead(myoPinLeft));  // Display EMG value
      Mouse.move(-pixelStep, 0); // Move cursor specified increment
      velDelta = (delayTime / ((analogRead(myoPinLeft) / myoLimitLeft)
* velScale)); // Cursor velocity control: scale movement delay by ratio
of reading over threshold
      delay(velDelta);
    }
    else if (analogRead(myoPinRight) > myoLimitRight)
    {
      Serial.println("Right");
      Serial.println(analogRead(myoPinRight)); // Display EMG value
      Mouse.move(pixelStep, 0); // Move cursor specified increment
      velDelta = (delayTime / ((analogRead(myoPinRight) /
myoLimitRight) * velScale)); // Cursor velocity control: scale movement
delay by ratio of reading over threshold
      delay(velDelta);
    }
    // Activate mouse "left click" when signal exceeds threshold for
left and right inputs. Multiplier is scale factor.
    if ((analogRead(myoPinLeft) > (myoLimitLeft*1.4)) &&
(analogRead(myoPinRight) > (myoLimitRight*1.4)))
    {
      Serial.println("Left Click");
      Mouse.click(MOUSE_LEFT); // Activate mouse left click
```

```
      delay(delayClick); // Button debounce delay (so don't click
multiple times)
    }
  }
}
```